IDENTIFICATION OF ALTERNATIVELY SPLICED MENKES COPPER ATPASE (*ATP7A*) TRANSCRIPT VARIANTS

By

CHANGAE KIM

A THESIS PRESENTED TO THE GRADUATE SCHOOL
OF THE UNIVERSITY OF FLORIDA IN PARTIAL FULFILLMENT
OF THE REQUIREMENTS FOR THE DEGREE OF
MASTER OF SCIENCE

UNIVERSITY OF FLORIDA

2011

To my wonderful husband without his endless love, prayer, encouragement and support, none of this would be possible

ACKNOWLEDGMENTS

There are many people who were there for me to complete this task. Without them I would not have been able to finish this work. I would like to first thank my advisor Dr. James F. Collins. Dr. Collins gave me this wonderful opportunity to explore in the scientific world. He has taught me how to do bench work, and how to write and speak in a scientific manner. I will always be thankful that he was my mentor. I would like to thank Dr. Ranganathan for helping me around the lab. I would like to thank the members of my committee, Dr. Mitchell Knutson, who would always challenge me and help me to think in depth and figure out the problem together. I also would like to thank Dr. Michelle Gumz, who was always there for me with warm heart, supporting me and encouraging me to finish strong. I thank my lab members (Lingli Jiang, Sukru Gulec, Yan Lu, and Liwei Xie) for their assistance, encouragement, and friendship. Lastly, I would like to thank my friends and family for all their support and love.

TABLE OF CONTENTS

page

LIST OF TABLES

Table page

LIST OF FIGURES

Abstract of Thesis Presented to the Graduate School
of the University of Florida in Partial Fulfillment of the
Requirements for the Degree of Master of Science

IDENTIFICATION OF ALTERNATIVELY SPLICED MENKES COPPER ATPASE (ATP7A) TRANSCRIPT VARIANTS

By

Changae Kim

December 2011

Chair: James F. Collins
Major: Food Science and Human Nutrition

The Menkes copper Atpase (*Atp7a*) protein is responsible for copper export from intestinal epithelial cells. The *Atp7a* gene is strongly induced in the small intestine of iron-deficient rats, suggesting an important physiological role during perturbations of iron homeostasis. Recent studies revealed novel 5' splice variants of the rat *Atp7a* transcript (1). Novel 5' splicing events have been documented but how those relate to potentially alternative transcripts is not clear. Methods: Forward and reverse primers were designed in the rat *Atp7a* gene, and RT-PCR was used to amplify different regions of the *Atp7a* cDNA, including the full-length transcript. Northern blotting was performed to quantify *Atp7a* mRNA expression in control and iron-deficient rats, and to identify the number of transcript variants that exist. Results: Full-length *Atp7a* transcripts containing the 5' splice variants were identified by PCR and Northern blotting. Northern blotting also clearly identified multiple *Atp7a* transcripts. Confirming previous qRT-PCR analyses, Northern blots showed increased *Atp7a* mRNA expression in iron deficiency. Conclusion: These results suggest the existence of multiple *Atp7a* transcripts in rat intestine, including full-length transcripts containing three 5' splice variants. Moreover, the induction of *Atp7a* gene expression was confirmed by a complementary method.

Further research is important to confirm the existence of alternative Atp7a proteins encoded by these splice variants, and to determine their intracellular location and to characterize their functional properties.

CHAPTER 1
INTRODUCTION

The metabolic link between iron and copper has been studied for decades. In fact, copper and iron are known to interact with each other in many ways, including absorption and intracellular transport. In 1928, Hart et al uncovered the relationship between iron and copper, specifically discovering the role of copper in forming hemoglobin and in overcoming anemia. (2, 3). Also, in 1980 there were studies on the effect of iron deficiency on copper metabolism during pregnancy and the interaction of these metals in pregnant animals (4). The results showed that iron deficiency caused an increase in the mother's liver copper level. In the fetus, as the iron content of the maternal diet decreased, the iron and copper liver levels also decreased (5). Furthermore, a rat study during the suckling period through adulthood showed that iron deprivation led to an increase of copper in enterocytes and liver (6). Further studies involving the metabolism of copper and iron may provide additional insight into the connection between these pathways and their physiological roles.

There is a biological importance for humans and other mammals of iron containing proteins. Iron dependent proteins that contain neither iron sulfur clusters nor heme, transiently bind iron and facilitate its movement across the plasma membrane and intracellular membranes. In animals, iron sulfur cluster containing proteins are linked by a series of enzymatic steps, and they are important for cellular energy production. The primary function of heme iron is to be the oxygen-carrying constituent of hemoglobin in erythrocytes and myoglobin in muscle tissue. These two proteins exemplify the importance of iron in mammalian physiology.

Iron physiology is important for normal homeostasis. On average, 3 to 4 g of iron is contained in an adult human. Approximately 2 g is found in the blood as hemoglobin iron. Iron is stored in liver, spleen and macrophages. Under normal circumstances, girls have 300 mg and women have 1000 mg of total body iron. Boys and men have higher amounts of stored iron with boys having 500 mg and men 1500 mg. However, under pathological conditions, iron stores can reach 40,000 to 50,000 mg (7). Iron is absorbed from the intestine or released into the circulation from macrophages during red blood cell (RBC) breakdown. After 120 days of circulation, senescent RBC, are scavenged and ingested by cells of immune system, known as reticuloendothelial macrophages. These macrophages are mainly found in the spleen, liver and bone marrow. Macrophages of the reticuloendothelial system (RES) in these tissues recognize senescent RBCs, ingest them, breakdown hemoglobin, and recycle iron back into serum. Most of the iron used for hemoglobin synthesis is supplied to the plasma transferrin pool by the RES. The ferric form of iron in plasma is carried by transferrin. Transferrin is an 80-kDa glycoprotein consisting of a singly polypeptide chain and two N-linked complex-type glycan chains (8). The total amount of iron bound to transferrin in the plasma is about 3 mg. Approximately 70-90% of the iron on transferrin is delivered to the bone marrow for hemoglobin synthesis in RBC precursors. However, about 20-25 mg of iron must cycle through the transferrin iron compartment daily to meet the ongoing needs of erythropoiesis.

There are many known physiological roles of copper. Copper has an essential role in cross linking of collagen and elastin, which is required for the formation of strong, flexible connective tissue. The cross linking of collagen is done by the copper

dependent enzyme lysyl oxidase. Rat studies have shown that lysyl oxidase activity decreases during severe copper deficiency (9). Copper also plays multiple roles in the central nervous system. The role of cuproenzymes in catecholamine metabolism implies a function in normal neurotransmission (10). The role of copper in cardiac function has been studied in the past. Weanling rats deprived of copper showed cardiac symptoms but no symptoms were apparent in older rats. In one study, humans with copper deficiency were shown to have irregularities in heart function (11). Furthermore, there are several studies showing a role for copper in immune function. An animal study has shown that both low and high copper intakes influence immune function. Animals with severe copper deficiency showed changes in T lymphocytes and T helper cells, B cells and monocytes, and interleukin 2 (12). There are other physiologic functional roles of copper, and the effect of dietary copper needs to be further investigated in the future.

On average approximately 1.3 mg/d of copper enters the body from the diet. Approximately 0.8 mg/d of copper is extracted from the diet and delivered to the liver. Excretion occurs mostly through the copper exporter ATP7B into the bile. In liver, copper is incorporated into ceruloplasmin (CP) and other cuproenzymes. CP is secreted into the circulation for copper delivery to cells of the body. Approximately 100 mg of total body copper content is distributed in various tissues, with most found in bone and muscle. Homeostatic control of body copper levels includes modulation of copper absorption in the intestine and copper excretion from the liver.

The Menkes copper ATPase (*Atp7a*) is a P-type Atpase, which is expressed in intestinal epithelial cells (IEC-6), where it is important for copper efflux after dietary absorption. The *Atp7a* gene is strongly induced by iron deficiency in the rat intestine (6).

Iron homeostasis related genes (e.g. *Dmt1* and *Dcytb*) are upregulated by HIF2α during iron deficiency in the mammalian intestine. The *Atp7a* gene is also upregulated by a direct interaction with HIF2α, demonstrating coordinate regulation with genes related to intestinal iron homeostasis (13). Recent studies also revealed alternative 5' splice variants of *Atp7a* in rat intestine and intestinal epithelial (IEC-6) cells (1). Utilizing an array of Atp7a antibodies, which were extensively validated, different Atp7a proteins were detected among proteins isolated from the membrane and cytosolic fractions. The specificity of the immunoreactions was confirmed by shRNA knockdown of *Atp7a* transcripts, with resulting attenuation of the bands detected in membrane preps (unpublished observation). Thus, alternative splicing of the *Atp7a* transcript may lead to the production of novel protein variants in potentially different subcellular locations with distinct functions.

Menkes disease is an X-linked recessive disorder of copper deficiency. A primary defect in Menkes disease is the reduced transport of dietary copper across the basolateral membrane of enterocytes to hepatic portal circulation. The gene affected in patients with Menkes disease was identified in 1993-94 by several research scientists (16). The gene that underlies this disease is called Atp7a. Atp7a is important for regulating copper levels in the body. In the small intestine, Atp7a protein helps control the absorption of copper from our diet.

To verify novel splice variants and to determine the number of *Atp7a* transcripts, we used intestinal epithelial cells in culture and rats fed an iron deficient diet. We hypothesized that multiple *Atp7a* transcript variants exist and that some of them contained novel 5' splice variations. The approach was to use a PCR based strategy to

identify splice variants. Also, Northern blot analysis was utilized to detrmine the number of *Atp7a* transcripts and to quantify gene expression levels during iron deficiency.

CHAPTER 2
LITERATURE REVIEW

Introduction to Copper

Copper is one of the required trace elements in humans and is an essential nutrient for all organisms. Copper is found in the body in two transition states, the oxidized cupric ion (Cu^{2+}) and the reduced cuprous ion (Cu^{1+}). There are several inhibitors that affect copper absorption, including phylate, zinc in excess, iron, calcium/phosphorus and vitamin C. In the gut, copper is absorbed by enterocytes before distribution to the body (14). Dietary copper absorption is dependent on the exporter Atp7a. An error can occur where Atp7a is mutated or dysfunctional, which leads to Menkes disease. The genetic defect in this disease was identified in 1962 (15), but more detail of the physiological role was discovered by several research scientists more recently. Menkes disease is an X-linked recessive disorder of copper deficiency, with a reported incidence of 1:10,000 live births (16). Patients with Menkes disease show dramatic developmental and neurological impairment due to disrupted delivery of copper to the brain. The majority of Menkes disease patients do not live past early childhood. Other symptoms that are caused by a decreased function of copper dependent enzymes are connective tissue abnormalities and lack of pigmentation.

The dietary recommendation for copper was first introduced in 1980 (17). An Upper Tolerable Intake Level (UL) has also been established as an excessive amount of copper can potentially be toxic. Obervations from in vitro cell culture studies have shown that excessive copper can lead to the presence of free cuprous ions that readily react with hydrogen peroxide, forming the deleterious hydroxyl radical, which can

damage DNA and other cellular biomolecules (18). Moreover, there are many other nutrients that can interact with copper and alter its cellular homeostasis.

Copper Homeostasis

Copper Intake and Requirement

Dietary reference intakes for copper were established almost a decade ago. The richest food sources of copper include shellfish, nuts, seeds, organ meats, wheat bran cereals, whole grain products, and chocolate foods. Other fruits and vegetables, chicken, many fish, and dairy products contain relatively low concentrations of copper (19). Depending on individual food choices, copper intake can vary daily. The Third National Health and Nutrition Examination Survey showed that the median intake in the United States is approximately 1.0 to 1.1 mg/day for women and 1.2 to 1.6 mg/day for men (20). This survey shows that healthy individuals are consuming higher amounts than the current RDA which indicates that in the United States, dietary copper requirements are met.

The Dietary Reference Intakes (DRI) for copper were established in 2001 (21). The RDA for adult males and females is 0.9 mg/day. The RDA for pregnant women is 1 mg/day and for lactating women is 1.3 mg/day. The DRI recommendations for children vary with age. Adequate intake (AI) for infants from 0 to 6 months of age is 0.2 mg/day and for infants from 7 to 12 months age is 0.22 mg/day. The Tolerable Upper Intake Limit (UL) for copper is 10 mg/day. This upper limit was created due to potential liver damage caused by excess copper. Haschke et al. have shown that infants consuming a diet high in iron may interfere with copper absorption (22). Infants fed a formula containing low concentrations of iron absorbed more copper than infants consuming the same formula with a higher iron concentration.

Copper Absorption

Our daily food intake is the main source of the copper for our bodies. The exact mechanism is not fully defined, but studies with animal models have begun to provide some basic information on the mechanism of copper absorption (23). 25-50% of copper found in the daily foods humans consume is readily absorbed by the small intestine. When a deficiency in copper occurs, there is an increase in copper absorption and the opposite occurs when copper is in excess, causing a decrease in absorption. Dietary copper must be reduced from the Cu^{2+} to the Cu^{1+} state for transport across the apical membrane into enterocytes. Once reduced, the metal is likely transported into enterocytes via facilitated diffusion by copper transporter 1 (Ctr1). Ctr1 is a homotrimeric plasma membrane protein that was first discovered in *Saccharomyces cerevisiae* and later characterized in mammals (24, 25). The human form of Ctr1 (hCtrl) was identified by complementation of a yeast mutant (Ctrl1) that is defective in high affinity copper uptake. The toxicity of copper overload was more pronounced with overexpression of the Ctr1 gene in yeast (25). In the homozygous Ctr1 knockout mouse, a higher amount of copper was found in the intestine of the KO compared to the wild type mouse (26), which suggests that copper import can occur without Ctr1.

Another possible transporter involved in copper absorption is divalent metal transporter (Dmt1). Dmt1 is known to transport iron across the apical membrane of enterocytes; Dmt1 can also transport Mn^{2+}, Cu^{2+}, Co^{2+}, Ni^{2+}, and Pb^{2+} (27, 28). Intestinal Caco-2 cell studies have shown the ability of Dmt1 to transport copper. Caco-2 cells were transfected with DMT1 antisense nucleotide, resulting in an inhibition of iron uptake by 80% and an inhibition of copper uptake by 47%. This result suggested that DMT1 is the main iron transporter but that it also participates in copper transport

(29). In a study of dietary iron deprivation, Dmt1 mRNA and protein levels were strongly induced (30). However, others have studied intestinal Cu import in Belgrade rats, a mutant rat with nonfunctional Dmt1, and described a novel ATP-dependent absorption process for copper (31).

Copper Handling by Enterocytes

Once copper is absorbed into the enterocyte, it is bound by chaperones that deliver it to several cuproenzymes, copper binding proteins, or the copper export protein Atp7a. Atox1is a chaperone for the Menkes copper ATPase (ATP7a), which delivers copper to the *trans*-Golgi network. Copper is transported out of enterocytes by Atp7a or other unknown proteins. Once copper exits enterocytes, the oxidizing environment converts cuprous copper (Cu^{+}), which specifically interacts with Ctr1 and Atp7a, to cupric copper (Cu^{2+}), which binds to albumin or α_2-macroglobulin for delivery in the portal blood to the liver (Figure 2).

Delivering to Liver

After release into the portal blood stream, copper bound to albumin or α_2-macroglobulin is taken up by the liver, either for storage, mobilization into the peripheral circulation, or excretion into bile. Some of the copper is incorporated into metallothionein (MT) in the liver of animals when copper intake is high, suggesting a role for MT in cellular detoxification (32). A large proportion of hepatic copper is incorporated into ceruloplasmin (CP) within hours, which is excreted into the blood. Ceruloplasmin accounts for over 80% of the copper found in the circulation, and contains 6 atoms of copper in its structure. CP with its bound Cu is released from the liver into the blood and is delivered to cells with specific CP receptors on their surface. Ceruloplasmin binds to these receptors; the copper is reduced, dissociates from CP,

and is released into the cell (33). Cp plays an important physiological role in iron release from sites of iron storage and in the central nervous system.

Copper Excretion

The primary route of copper excretion is through bile into the gastrointestinal tract. During copper loading, the Atp7b copper ATPase translocates to the biliary canalicular membrane for copper export and excreted copper combines with a small amount of copper from intestinal cells, pancreatic and intestinal fluids, and unabsorbed dietary copper. This copper is then eliminated in the feces (34). Fecal copper is the major excretory route, and about 97% is lost, with only a small amount being reabsorbed. Healthy humans excrete only 10 to 30 µg of copper per day in the urine, but urinary losses can increase markedly in some conditions, such as renal tubular defects (35). Other routes of excretion include saliva, hair, nails, and sloughed epithelial cells; however, they contribute little to total copper loss. Atp7b also pumps copper into the *trans*-Golgi network in hepatocytes for incorporation into *apo*-ceruloplasmin prior to secretion into the peripheral blood system. The genetic defect of the *Atp7b* gene will result in Wilson's disease, which is an autosomal recessive disease that causes abnormal copper storage in body tissues. Copper chelation therapy using D-penicillamine is available for treatment of Wilson disease; this therapy is not always successful, especially if diagnosis is delayed and it may have severe side effects. When there is copper accumulation in the liver, brain and kidney, multi-organ damage occurs, including liver dysfunction, movement disorders, cirrhosis, and neuropsychological abnormalities (36).

Iron Homeostasis

Iron Absorption

In our body, two-thirds of the iron is found in hemoglobin within red blood cells (RBCs). RBCs circulate for 120 days, and are ingested by immune system macrophages. These macrophages are found in the reticuloendothelial system (RES) which recognizes old RBCs, ingests them, and breaks down the hemoglobin. Furthermore, the RES liberates the iron and recycles it back into the bloodstream. Our dietary iron is absorbed in the upper small intestine, predominately in the epithelial cell layer of the duodenum and proximal jejunum.

Iron is a dietarily essential transition element. Ferrous iron, Fe^{+2}, is the biological form of iron found in humans and other mammals. However, most of the food we consume contains the ferric form (Fe^{3+}), which is highly insoluble. Before it can be efficiently absorbed, the ferric iron needs to be reduced to the ferrous form (Fe^{2+}). Iron enters the plasma bound to transferrin, which is involved in transporting iron between tissues and around the body. Transferrin will move to the duodenum, which is a major player in iron metabolism because this tissue is where iron is absorbed and delivered into the portal circulation. Circulating transferrin bound iron is taken up into cells by a cell surface transferrin receptor by endocytosis. The slightly acidic environment in the endosome releases Fe^{3+} from transferrin, which is then reduced to Fe^{2+}. The Fe^{2+} is then transported out of the endosome by divalent metal transporter 1 (DMT1). In the duodenal enterocyte, divalent metal transporter 1 (DMT1) is also the main transporter for intestinal iron uptake (37). A mutation of Dmt1 may cause iron deficiency anemia. In studies where *Dmt1* was knocked out in the small intestine (27), and in rodents carrying

spontaneous mutations in *Dmt1* (38), animals were severely anemic. These findings suggest that Dmt1is likely the major route for iron transport into the enterocyte.

One of the brush border reductases that can act on ferric iron is duodenal cytochrome b (Dcytb) (39). Dcytb expression is highest in the proximal small intestine, and during iron deficiency or in hypoxia, its expression is enhanced by stimuli that increase iron absorption (40). However, in a recent study, Dcytb knockout mice had no clear phenotype which shows that Dcytb is not essential for iron absorption (41). Other reductases may thus be involved (42).

Absorbed iron then enters the labile iron pool along with any absorbed heme iron and is available for use by the cell or export out of the cell by ferroportin. Ferroportin (Fpn1) is the only known exporter of iron and is required in order for iron to cross the basolateral membrane into the portal circulation. Ferroportin is induced by iron deficiency when iron absorption increases. The importance of Fpn1 has been shown by deletion of the gene in zebrafish, mice, and by mutation of the gene in humans (43-45). Intestine specific knockout of Fpn 1 led to severe iron deficiency, and zebrafish lacking Fpn1 also showed severe iron deficiency. These findings suggest that Fpn1 is required for normal iron absorption. Iron efflux from the enterocytes also requires Hephaestin (Heph). In the small intestine, Heph plays a role as a major iron oxidase. Heph was identified by positional cloning as the gene mutated in the sex-linked anemic (*sla*) mouse (46). Hephasestin has high homology to the plasma protein ceruloplasmin (CP). Heph shares with CP an ability to bind copper and an ability to oxidize ferrous iron to ferric iron.

Iron in Liver

In iron metabolism, the liver plays an important role. Hepatocytes and Kupffer cells are the long term depository for iron. Most importantly, the liver synthesizes hepcidin (Hepc) and secretes it into the circulation to regulate systemic iron metabolism. Hepc is a negative regulator of iron absorption in the gut and iron release from storage sites. When body iron increases, the liver produces hepcidin, causing ferroportin to be internalized and degraded by interaction with Hepc, which in turn inhibits iron transport across the intestinal epithelium into the portal blood (47). In one study using mice that lacked Hepc, the animals developed significant iron overload (48). This result demonstrates that hepcidin is inversely related to body iron intake. Furthermore, a study where mice were engineered to overexpress hepcidin showed that these mice developed a severe iron deficiency anemia (49). This result showed that hepcidin was a repressor of iron absorption, so iron absorption is increased when hepcidin levels are reduced as in iron deficiency.

Copper and Iron Interactions

Dietary iron and copper are absorbed in the duodenum, where interaction occurs. Once copper is in the cell, it is delivered to Atp7a. During iron deficiency there is increased metallothionein (MT) mRNA expression and Atp7a mRNA and protein expression, which suggests that copper absorption, may be increased during states of iron deficiency. Absorbed copper is transported by albumin or α_2-macroglobulin in the portal blood to the liver. In liver, copper is incorporated into the ferroxidase, ceruloplasmin (CP), or excreted into the bile. In order for iron to be released efficiently from hepatocytes and other tissues, CP is required. Results in CP KO mice have shown that iron accumulates in hepatocytes (50). Copper is released from the liver bound to

CP. Ceruloplasmin functions to deliver copper to other organs and tissues, and as stated it is also important for iron release from certain tissues. Iron bound to TF delivers iron to the bone marrow for red cell hemoglobin production; iron utilization by these cells is copper dependent. Even though copper deficient mice have sufficient amounts of plasma iron, the mice still become anemic because copper deficiency affects iron utilization by erythroid cells. This defective iron utilization may affect hemoglobin synthesis. Iron is also taken up by other tissues, but in brain, iron release is dependent upon glycosylphosphatidylinositol-linked CP (PI-CP). In rats given a copper deficient diet, the iron concentration is lower in brain (51). Iron contained within erythrocytes is recycled to reticuloendothelial (RE) macrophages. The release of iron from RE macrophages is a copper dependent process, again involving CP and GPI-CP (42). Moreover, dietary copper deprivation causes CP deficiency, which causes iron to accumulate in the RE cells (50). This CP deficiency in RE macrophages highlights the recent discoveries of the connection between copper and iron.

The discovery of genes and gene mutations involved in the metabolism of copper and iron will provide an important key to a deeper understanding of the connections between the pathways, and their physiological and pathological consequences. The connection of copper and iron was reported in 1928 by Hart, Elvehjem et al. (2). They first showed that copper can facilitate hemoglobin formation and overcome anemia. In 1932, the retention of iron and its partition between the hemoglobin and the tissues was studied in rats. The rats were fed milk alone or 0.5 mg of iron per day or 0.1 mg/day of Cu was added to the milk. The results showed, when extra iron was given, it was divided between hemoglobin and the tissues. When extra copper was given, a large

amount of the retained iron went to the bone marrow for hemoglobin formation and the tissue iron was reduced (52), suggesting that copper has no effect on iron retention.

A recent review highlights current advances in iron-copper interactions for regulating iron and copper homeostasis (42). During iron deficiency increases of copper in enterocytes has been noted. An in vivo study has shown increased mRNA expression of metallothionein (MT) and *Atp7a* mRNA in rats that were fed an iron deficient diet (1, 6), again suggesting increased copper content in intestinal enterocytes. A monolayer of polarized Caco2 cells, which models intestinal mucosa, was used to compare the effects of Fe^{2+} and Cu^{2+} on cellular uptake and overall transport. The depletion of cellular iron or copper have increased uptake of both metal ions, and also enhanced overall transport of iron from the apical to the basal chamber. This study suggested that perhaps copper availability in some way influences the expression of transporters associated with basolateral iron transport (23).

In iron- deficient rat intestine, the *Atp7a* gene is strongly induced, suggesting increased copper absorption by enterocytes (6). The relationship between iron and copper absorption and storage has been studied for decades. In one study, rats were fed a milk diet deficient in both Fe and Cu, and replenished with either copper or physiological saline solution. This study showed that rats that were administered copper had a significantly higher concentration of iron in the plasma than the group given saline. This result supports the theory that copper is necessary for the release of iron from storage sites (53). Moreover, a current study utilizing gene chip analyses revealed genetic changes in the duodenum during iron deficiency. The results showed that several different genes were induced, and one of the most interesting genes was the

Menkes copper ATPase (*Atp7a*) (54). Atp7a may be involved in the hepatic copper loading observed during iron deficiency and might play important roles in overall body iron homeostasis (30). In a rat study from the suckling period through adulthood, novel genes involved in iron absorption during iron deficiency were identified. In this study, Menkes copper ATPase (*Atp7a*) showed strong induction in iron deprived rats of all ages examined, which provided evidence that may explain copper loading in the iron deficient state (6). The induction of *Atp7a* in iron deficiency was also replicated in an in vitro model, IEC-6 cells. Three splicing variants were shown to be strongly induced during iron deprivation in these cells (1). These ongoing discoveries provide an important key to a deeper understanding of connection between iron and copper.

Menkes Copper ATPase (*Atp7a*)

The Menkes Copper ATPase gene is P-type Atpase that delivers copper to cuproenzymes in the secretory pathway and is used for cellular copper export. Dierick et al. reported a detailed molecular analysis of the genomic structure of the Menkes disease gene. There are 23 exons in *Atp7a*, covering a genomic region of approximately 140 kb (55). This Menkes P-type ATPase is predominantly localized to the *trans-Golgi* apparatus of cells. Atp7a continuously recycles between the Golgi and the plasma membrane when copper efflux occurs. Based on the dynamic role of the *trans-Golgi* network in cellular protein trafficking, we can further understand the role of Atp7a in copper efflux from the cell (56).

However, there are many splice variants that are found during genetic mutations and splicing of normal physiological relevance. Gene splicing occur in eukaryotes, prior to mRNA translation, by the differential inclusion or exclusion of region of pre-mRNA. Gene splicing is an important source of protein diversity. The pre-mRNA transcribed

from one gene can lead to different mature mRNA molecules that generate multiple functional proteins. Splice variants can be trafficked to different places and can function differently under different circumstances. Gene splicing enables a single gene to increase its coding capacity, allowing the synthesis of protein isoforms that are structurally and functionally distinct.

Studies have verified that three splice variants of *Atp7a* are found in rat intestinal epithelial cells (1). Alternative splicing is now thought to affect more than half of all human genes (57). Protein function can be regulated by the removal of interaction or localization domains by alternative splicing. Also, this process can regulate gene expression by splicing transcripts into unproductive mRNAs targeted for degradation. Splicing variants can thus be thought of as on/off switches that can regulate gene expression (58). By affecting regions involved in interaction or localization, alternative splicing may generate alternative protein isoforms that could play key regulatory roles (57). Alternative splicing machinery is thus an efficient tool for protein and gene expression regulation.

During genetic mutations in humans and rats, Menkes disease often presents splicing mutations associated with partial skipping of the exons (59). After amplifying cDNAs from different human cell lines, sequence analysis revealed that multiple transcripts of *Atp7a* were present. One of the splice variants was 5 kb and it was missing exons 3-15 (60). This splice variant was considerably smaller than the 8.5 kb full-length Atp7a mRNA (55).

Also, there is splicing variant study using a mouse model. Mice hemizygous for the blotchy allele of the X-linked mottled locus have similar connective-tissue defects

known as occipital horn syndrome (OHS) and may represent a mouse model of this disease. This disease also has abnormal of copper transport and is known to be allelic to Menkes disease. This study with blotchy mice showed that northern blot analysis revealed the presence of three transcripts, one of normal size and two > 8.4 kb mRNA (59). In addition, by screening patient samples for mutations by RT-PCR and by the chemical cleavage-mismatch technique, Das et al. recently identified 10 different mutations associated with classic Menkes disease.

Splicing of normal physiological relevance in the *Atp7a* transcript was detected in intestinal epithelial cells and rat intestine, by 5'RACE experiments; three splice variants were discovered (1). These observations lead to the conclusion that Atp7a protein variants may exist, with potentially different intracellular locations and distinct physiological functions. Many scientists are finding different splicing variants, yet characterization of these variants has not been completed in many cases. Uncovering what factors control splicing could be critical to provide additional insights into the mechanism of copper and iron homeostasis.

Importantly, our preliminary studies have indeed identified different sized Atp7a immunoreactive proteins, using an array of Atp7a antibodies and shRNA knockdown in IEC-6 cells with concomitant reduction of the immunoreactive proteins shown with western blotting (Lu, Y. & Collins, J. unpublished data). These current studies were thus designed to identify the transcript variants that encode these proteins, and to determine the total number of transcript variants that exist in intestinal epithelial cells.

Specific Aims

Specific Aim 1: Identifying different transcripts is an important step to verify the existence of novel splice variants. A complimentary PCR based approach using Exon 1

forward and exon 23 reverse primers was completed to produce the full-length *Apt7a* transcript. Also, a PCR based approach using different primer sets (Table 2) was completed to identify more novel splice variants. An alternative PCR based approach using Ex1-1A/23, Ex1-2/23, and Ex1-3/23 5'/3' primer sets was also used to identify potential splice variants.

Specific Aim 2: In order to determine the number of transcripts that exist in intestinal epithelial cells and whether *Atp7a* mRNA is regulated by iron status *in vivo*, the Northern blot technique was used. Total RNA was purified from rat duodenual mucosa and IEC-6 cells, and separated by gel electrophoresis. Probing was done using a non-radioactive technique using a full-length *Atp7a* cDNA clone to produce random prime labeled probes. Also, oligonucleotide 3' end labeling with digoxigenin-ddUTP probe was done. As some transcripts may be similar in size, different percentage gels were used and some gels were run for longer periods of time to separate large mRNA molecules of similar molecular weight.

Table 2-1. Rat Atp7a primer sequences chosen for the PCR

Exons	Forward Primers (5'→ 3')	Reverse Primers (5'→ 3')
Exon 1	AGGCTGCGTGCTGGTTGATC	
Exon 2	GGAATGTAAAGACATCAAAATGGAACC	TTAATGTGATGGACACCATTCACTTTC
Exon 3	ACTTCAGACTCCAAAGACCCTCCA	AA TGCGTTGTACACCTTGCAGCT
Exon 4		CAGCATCAAATCCCATGTCTTCAA
Exon 5	AGCCACTGGTCGTGATAGCTCAG	
Exon 6		AATGCCATTGCCTTCTCCAGC
Exon 7	TGACGTGTGCCTCCTGTGTCC	
Exon 8		TTATGATCTAAGTGGTTGGCTGATCG
Exon 9	GGACTGATGATCTATATGATGGTTATGGA	
Exon 10		CTTCGCTATGTGTTCCAGCCATC
Exon 11	AAGCTAATTTCCTTACAAGCAACAGAAG	
Exon 12	GAAGAACAAGTGGATGTGGAACTTGTA	GGACTCGTCTACCATAGAATGCCC
Exon 13	CCTGTGGCTAAGAAACCTGGCA	TGATGTCTGTGCCTCCTCTACAAGTT
Exon 14		GGAAAGTAGGCTTCCACAATTTCAA
Exon 15	GCTACAACAGAAGCATCTCCCGA	
Exon 16		TCCTAAAGGATGTTCACTGTTACTTTCTG
Exon 17	GTACCTGCACAGATTTCCAGGTTGTA	
Exon 18	TTCTGCTCTTCCTGTATTAGATGAACTGT	CTGAGAAGCAATAGACCGAGCTGTT
Exon 19		
Exon 20		AGCTGCTTCGATGGCTACATCTG
Exon 21	TGACCTTCTGGATGTTGTGGCA	
Exon 22		AGTACCACAGAGACAGATGAAGCGG
Exon 23		ACATAATGCCAGGTTCAGAGCTCC
3'end revII		CAGTGTGGTGTCGTCATCTTCCC
Exon 1/1A	TGGAATCCTAGACAGAATCTCACTAT	
Exon ½	CCTGGAATCCTAGGAATGTAAAGACA	

Table 2-1. Continued

Exons	Forward Primers (5'→ 3')	Reverse Primers (5'→ 3')
Full- length for Primer walking	ACCTCAAATTGGGAGCCATTGA	ACAAGACCATTTCTAATCATCCATTCC
Full- length2 for primer walking	ATCAGCACCACTAGATCATAAACGAA	TTAGGAGTTACATAGTGCTCTGTGCT

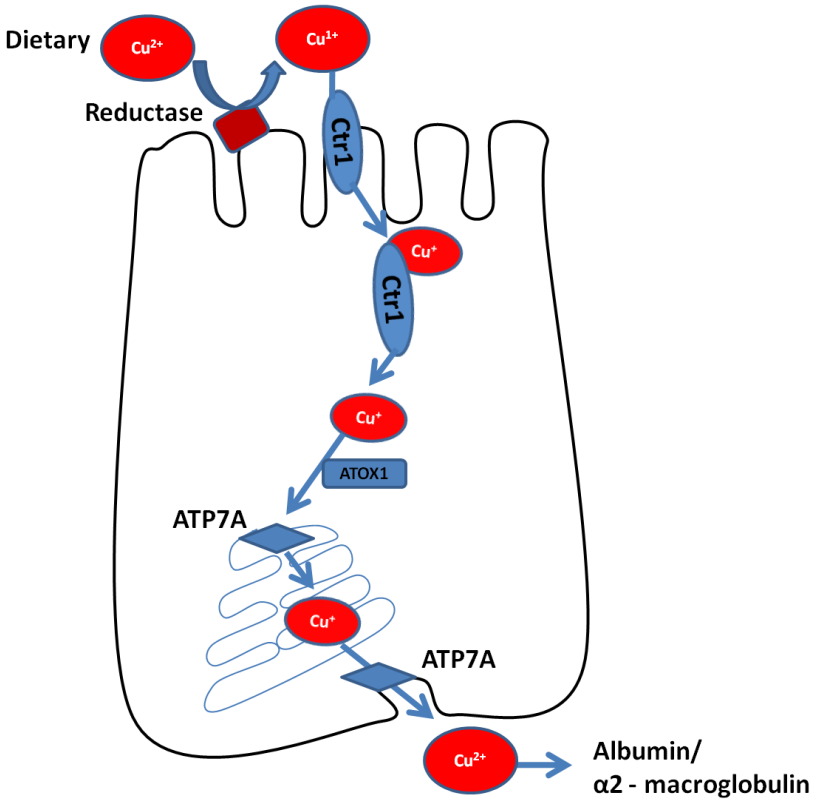

Figure 2-1. Process involved in a copper absorption Shown in this diagram is a single enterocyte, with the processes that are involved in copper absorption from the diet. Dietary copper is first reduced and then transported across the apical surface by copper transporter 1 (ctr1). Once copper enters the cytoplasmic pool, it is rapidly bound to chaperones for distribution to various cellular compartments. Copper chaperone atox1 delivers copper to the menkes copper transporting atpase (atp7a) in the *trans*-golgi network (tgn). In the tgn, copper is incorporated into copper containing proteins bound for the secretory pathway, including hephaestin (hp), a multi-copper ferroxidase that is important to oxidize transported iron on the basolateral surface for binding to transferrin. Under the conditions of copper excess, atp7a trafficks to the basolateral membrane and functions in copper export. Once cuprous copper exits cells, it spontaneously oxidizes and is then bound by albumin and α2-macroglobulin for transport through the portal blood to the liver. The copper export process may also be increased during iron deficiency, as atp7a expression is strongly induced.

CHAPTER 3
MATERIALS AND METHODS

Overview of Study Design for Specific Aims I and II

For specific aim 1, once intestinal epithelial cells (IEC-6 cells) reached 70-80% confluency, RNA isolation was completed. Using total RNA, RT PCR analysis was performed in a BIORAD Thermal Cycler. The forward primers and reverse primers were designed using PREMIER Biosoft NetPrimer, and by using different combination sets of primers, PCR was completed. The amplicons were visualized by agarose gel electrophoresis and PCR products were column purified. Purified PCR products were subcloned into T/A vectors and sequenced. Sequences were compared with databases to align the sequences with known cDNAs. For specific aim II, the same IEC-6 cells from specific aim I were used. Sprague Dawley rats were used as our animal model. The rats were fed control or iron deficient diets and mucosal scrapes were obtained after euthanization. RNA isolation was completed and total RNA was electrophoresed in different percentage agarose gels. The Northern blot procedure was completed next using ROCHE DIG high prime DNA labeling and detection starter kit II protocol. Also, oligonucleotide 3'end labeling with digoxigenin-ddUTP was done.

Chemicals, Reagents, and qPCR Primers

Chemicals were obtained from Invitrogen, Fisher Scientific, Fermentas, and Sigma Aldrich, and were of analytical grade or high purity. T/A cloning products were from Promega, Madison, WI. qPCR primers were from IDT, Coralville, IA. Other sources are mentioned as appropriate.

RNA Isolation from Rat Intestinal Epithelial Cells (IEC-6 cells) and Sprague Dawley (SD) Rats Intestine

All animal studies were reviewed and approved by the University of Florida IACUC. Male SD rats were obtained at 3-wks-of-age and were placed in wire mesh bottom cages, 1-2 animals per cage. Rats were fed AIN-93G diets (Dyets, Bethlehem, PA) that were either control (198 ppm Fe), or low iron (~3 ppm Fe). When rats were ~8 wk of age, they were euthanized and mucosal scrapes were taken from ~20 cm of the proximal small intestine. RNA was purified from mucosal scrapings and IEC-6 cells with Trizol reagent (Invitrogen, Carlsbad, CA), and quality was confirmed by agarose gel electrophoresis. RNA was quantified by a BIORAD NanoPhotometer. RNA samples were either fresh or stored in ethanol at -80^{o} C until use.

RT PCR Analysis Using the Rat Intestine and IEC-6 Cells Total RNA

To synthesize first-strand cDNA from total RNA, five micrograms of total RNA was reverse transcribed with SuperScript III First-Strand Synthesis System for RT-PCR (Invitrogen, Carlsbad, CA). Olidgo(dT) primer was used, and we followed the protocol provided by Invitrogen. Synthesized cDNA were either fresh or stored at -20^{o} C until use.

PCR Studies of *Atp7a* Splice Variants in Rat Intestine and IEC-6 Cells

To verify the presence of the detected splice variants and to determine novel splice variants at the 5'end, a PCR strategy was devised. PCR primers were designed as follows: Forward primers were designed in rat *Atp7a* exons 1, 2,3,5,7,9,11,12,13,15,17,18,and 21. Reverse primers were designed in rat *Atp7a* exons 2,3,4,6,8,10,12,13,14,16,18,20, 22, 23. (Table 2). Forward primers were also designed in rat *Atp7a* that bound to the exon 1/exon 1a junction; exon 1/ exon 2 junction; exon 1/

3 junction. These 3 primers were used with an exon 23 reverse primer, to verify the presence of the detected splice variants in full-length transcripts. All other primers were used in combination with a single forward primer and a single reverse primer, and all primers were designed to have similar melting temperatures. Two microliters of the cDNA reaction was used with Takara Ex Taq polymerase (Japan). Reactions were run in 200 microliter PCR tubes with the following cycling parameters: 94^{o} C for 2 min, 45 cycles with 94^{o} C for 30 s, 58^{o} C for 30 s, 72^{o} C for 4.5 min and then 72^{o} C for 10 min. The final PCR products were visualized by agarose gel electrophoresis. Exon 1 forward and exon 23 reverse primer set was used to amplify the full-length sequence for a template to generate probes for Northern blotting. Using the PCR products, cloning was done using the TOPO Cloning Kit (Invitrogen). Following ligation, transformation was completed using One Shot Top10 chemically competent cells (Invitrogen). 200 µl of transformation products were spread on ampicillin plates containing IPTG/ Xgal and incubated overnight at 37^{o} C. White colonies were chosen and removed from plate; these were grown in 5 ml LB medium overnight at 37^{o} C. The colonies were purified using the PureYield Plasmid Miniprep System (Promega). From these plasmid preps, 2 µg was sent out for sequencing to the University of Florida DNA Sequencing Core. A series of forward and reverse primers was used to sequence the full-length *Atp7a* cDNA fragment in its entirety by a primer walking strategy (Table 2).

Column Purification and Cloning

To clone the PCR product, A-tailing reaction was done as follows. 0.5 µl dNTP and 2.0 µl Taq polymerase was added and the mix was incubated at 37^{o} C for 15 min. Following the A-tailing reaction, column purification was performed by using GeneJet

PCR Purification Kit (Fermentas). The purification protocol provided by Fermentas was used. During the step of adding elution buffer, 30 µl of elution buffer was used. Following the purification, PCR amplicons were subcloned using a pGEM-T cloning vector (Promega). The cloning was done according to the procedure of pGEM-T Vector System I, using homemade DH5α bacteria as competent cells. TFB I and TFB II buffers were prepared before making competent cells. The composition of the TFBI buffer was as follows: 30 mM KAc, 100 mM KCL, 10 mM $CaCl_2$, 50 mM $MnCl_2$, and 15% glycerol. To sterilize, TFB I was filtered through a 0.22 µm filter unit (MILLIPORE) and stored at 4^o C. The composition of the TFB II buffer was as follows: 10 mM Na-Mops (pH 7.0), 75 mM $CaCl_2$, 10 mM KCl, and 15% glycerol. The buffer was autoclaved and store at 4^o C. First, the bacterial cells were streaked on a new LB plate and incubated overnight at 37^o C. Isolated colonies were selected and cells were precultured in 5 ml LB broth overnight at 37^o C. Next, 1 ml of cultured cells were inoculated into 100 ml LB broth and incubated for 2.5-3.0 hours at 37^o C, using a shaking incubator. The cells were asceptically transfered to sterile, ice-cold 40 ml centrifuge tubes, and the cultures were cooled to 0^o C by storing the tubes on ice for 5 min. Next, the cells were centrifuged at 4500 x g for 10 min. at 4^o C. The media was decanted from the cell pellets. The pellets were then resuspended in 10 ml of ice-cold TFB I and stored on ice for 10 min. Once again, the suspension was centrifuged at 4500 x g for 10 min at 4^o C, and the buffer was decanted from the cell pellets. The pellets were resupsended in 4 ml of ice-cold TFB II and stored for 15 min. on ice. 100 µl of this suspension was aliquot into prechilled tubes and frozen in on dry ice. Finally, the samples were stored at -80^o C for future use. Cloned PCR

products were sequenced utilizing vector specific primers. Sequences were compared with databases to align the sequences with known cDNAs (BLAST).

IEC-6 Cells Transfection with CFP Vector

We next sought to overexpress full- length *Atp7a* transcripts by transfecting IEC-6 cells, because these cells have been described to be a suitable in vitro model. IEC-6 cells were cultured under standard conditions in a humidified incubator in the presence of 5% CO_2 at 37^{o} C. Cells were grown in six well plates and transfection was performed when they had reached ~70% confluency. For cell transfection, TurboFect in vitro Transfection reagent (Fermentas) was used. In each well, 4 µg of DNA was diluted in 400 µl of serum-free 1X DMEM, 6 µl of Turbofect was added and cells were incubated with this mixture at 37^{o} C for 36 to 48 hours in a CO_2 incubator.

qPCR to Confirm the Over Expression of Atp7a Full-Length and Novel Splice Variants

The same primer sets were used as described above. Primers that amplified 18S rRNA were utilized as constitutive controls. RNA was purified from IEC-6 cells. RNA was converted to cDNA with the BioRad iScript kit in a 20 µl reaction with one µg of RNA. 2 µl of the cDNA reaction was used with 10 µl of SYBR Green master mix (BioRad) and 0.75 µl of each primer (3.33 pM each) in a 20 µl reaction. PCR cycling parameters were 50^{o} C for 2 min, 95^{o} C for 8.5min, and 42 cycles with 95^{o} C for 30 s and 60^{o} C for 1 min. Each RT reaction was analyzed in duplicate for 18S rRNA and Atp7a of IEC-6 cells.

Northern Blot for Gene Expression of Different Splice Variants and Identification of More Novel Splice Variants.

Northern blot analysis was performed according to the procedure of DIG High Prime DNA labeling and Detection Starter Kit II from ROCHE. Five micrograms of total RNA was electrophoresed in different percentages of agarose in 1X MOPS buffer containing 2% formaldehyde. After separation, the gel was soaked in 20X SSC twice for 15 minutes. Capillary transfer was allowed to proceed overnight in 20X SSC. The following day, the RNA was crosslinked onto a nylon membrane in a XL1000 UV crosslinker (Spectronics Co.) under the "optimal crosslink" setting for 60 seconds. Generation of DIG labeled probes was performed using the DIG High Prime DNA Labeling and Detection Starter Kit II (ROCHE) with 1 microgram of template DNA. The template DNA was the full- length *Atp7a* cDNA cut out of the plasmid vector and gel purified. The production of the full- length *Atp7a* cDNA is described above. The template DNA was diluted into double distilled water to a final volume of 16 µl in a reaction vial, and heated in boiling water for 10 min. The DNA was snap cooled on ice for 1 min and then added to the reaction tube. Four microliters of DIG High Prime (ROCHE) labeling mixture was added and mixed into the tube by pipetting. The reaction was incubated at 37^{o} C for 5 hours and then stopped by addition of 2 µl 0.2 M EDTA. A nylon membrane containing the RNA samples to be probed was prehybridized in DIG Easy Hybridization (ROCHE) solution at 42^{o} C for at least 30 min. The labeled probe DNA was denatured in boiling water for 5 minutes and then added to the hybridization tube. Hybridization continued overnight at 42^{o} C. The following day, blots were washed at 42^{o} C two times for 15 minutes in a wash solution (2X SSC, 0.1% SDS) in a shaking water bath, and subsequent washes were at 68^{o} C two times for 15 minutes (0.5X SSC, 0.1% SDS) also

in a shaking water bath. Following the washes, blots were exposed to Blue Basic Autorad film for the appropriate length of time. To determine the band size on films, the RNA ladder bands in the gel were measured from the top of the gel and a standard curve was made. Next, the distance that the band traveled on the film was measured and compared against the standard curve to estimate the size.

3'-End Labeling of Exon 1/1a, 1/2, and 1/3 Oligonucleotides

3'end labeling is the process of labeling oligonucleotides with digoxigenin-ddUTP (ROCHE) on the 3'end base. The following oligonucleotides were labeled: Exon 1/1a: 5'-TCGAACCCCAGCCCTGGAATCCTAGACAGAATCTCACTATGTCACCTATG-3'. Exon 1/2: 5'-TCGAACCCCAGCCCTGGAATCCTAGGAATGTAAAGACATAAAAATGGAAC-3'. Exon 1/3: 5'-CCCAGCCCTGGAATCCTAGGTTTCCCTAGAAGAAAAAAGTGCAACTGTTA-3'. These primers were designed to span different 5' exons. Using DIG oligonucleotide 3'-End Labeling Kit, 100 pmol of oligonucleotide was added to sterile double distilled water to make a final volume of 10 µl. The tube was placed on ice and the following reagents were added: 4 µl of reaction buffer, 4 µl of $CoCl_2$ solution, 1 µl of DIG-ddUTP solution and 1 µl of terminal transferase. Samples were mixed, centrifuged briefly and incubated at 37^{o} C for 15 min. After the incubation, samples were kept on ice. 2 µl of 0.2 M EDTA was added next to stop the reaction, followed by hybridization to the membrane. 20 ml of DIG Easy hybridization solution was preheated. The blot was incubated in heated hybridization solution for 30 min. 5 pmol of the end-labeled probe was added in 3.5 ml of fresh DIG Easy hybridization solution. The prehybridization solution was poured off and the probe/DIG Easy Hybridization mixture was immediately added to the

membrane. The mixture was incubated with gentle agitation for 13 hours at 43^{o} C. There were two step post hybridization washes. First, the membrane was washed 2 times for 5 min in 2 X SSC + 0.1% SDS at 42^{o} C. Next, the membrane was washed 2 times for 15 min in 0.5 X SSC + 0.1% SDS at 68^{o} C. There was constant agitation while the membrane was being washed. After the washes, blots were processed identically as described in the previous section.

CHAPTER 4
RESULTS

Identification of Different Splice Variants by Using PCR

In order to identify different splice variants, we designed different forward and reverse primer sets and used them for RT-PCR (Table 2). First, the quality of the RNA was assessed by loading 2 µg of total RNA into a 1% agarose gel. The gel confirmed that the RNA was of high quality (Figure 4-1A). Moreover, 18S rRNA was analyzed to provide further evidence of RNA quality (Figure 4-1B). Furthermore, exon 1 forward and exon 3 reverse primers were used to examplify successful production of the cDNA; this fragment from the 5' end of the *Atp7a* transcript was successfully amplified demonstrating the quality of the cDNA produced (Figure 4-1C).

To amplify the *Atp7a* full- length transcript, IEC-6 cell cDNA was used for RT-PCR with exon 1 forward and exon 23 reverse primers. The size of the full- length *Atp7a* transcript is approximately 4.6 kb, which was confirmed by agarose gel electrophoresis (Figure 4-2). Moreover, by using different forward and reverse primer sets, PCR demonstrated that exon 1-6 amplification produced multiple bands (Figure 4-3A). Also, exon 7-10, 13-16, 17-20, 18-22, and 21-23 amplification showed multiple bands (Figure 4-3B). The common forward and reverse primers were used here as a positive control. This procedure was done using RNA purified from IEC-6 cells. By using RNA from rat intestinal mucosal scrape, the PCR was also done with 5'end primers and different reverse primers. Exon 1-6, 1-8, 1-10, 1-12 and 1-14 amplification showed multiple bands (Figure 4-4A). Furthermore, again by using RNA from IEC-6 cells, additional PCR reactions were done with 5' end primers and different reverse primers. Exon 1-20, 1-22, and 1-23 amplification showed multiple bands. After cutting out each band from the

gels, amplicons from exon 1-23 were cloned into a T/A vector and sent out for sequencing (Figure 4-5). These PCR experiments showed that there are potentially several different splice variants of the *Atp7a* transcript.

Verification of Known Splice Variants

A previous study in rat intestine and intestinal epithelial cells in culture revealed splice variants of *Atp7a* by using 5'rapid amplification of cDNA ends (RACE) (1). The current studies were thus designed to verify the existence of these alternative splice variants. The previously identified gene structure and the relative location of PCR primers used are shown in (Figure 4-6). The exon 1/1a, 1/2, and 1/3 primers were designed to span different 5' exons (Table 2-1). Using these primers with exon 23 reverse primer, PCR indicated three solid bands (Figure 4-6B). These were sub-cloned and sent out to be sequenced to confirm that these are the correct gene.

A different technique was also used to identify more novel splice variants. Total RNA was isolated from SD rat mucosal scrape. The rats were either on a control diet or iron deficient diet. To measure the size of the different bands, a standard curve was made by using an RNA ladder (Figure 4-7A). The total RNA was loaded in the gel and transferred to a nylon membrane. The blot was probed with *Atp7a* full- length, and the blot showed different sized bands (Figure 4-7B). Exon 1/1a, 1/2, and 1/3 oligonucleotides were designed to label the 3'ends with digoxigenin-ddUTP. In control experiments to validate probe labeling, the film revealed the intensity of the spots to determine the amounts of DIG-labeled oligonucleotide in our samples (Figure 4-8A). Total RNA was loaded on the gel and transferred to a nylon membrane. The blots were probed with either full-length *Atp7a* probes or oligonucleotides 3'end labeled (ex1/1a,

1/2, and 1/3); although there is a lot of background, an identical pattern was observed using full-length probe vs. the different oligonucelotides (Figure 4-8B).

Gene Expression of Different Splicing Variants

A previous study using qRT-PCR has shown that the *Atp7a* gene is strongly induced by iron deficiency in the rat intestine (6). By performing Northern blots, we were able to confirm the induction of the *Atp7a* gene in iron- deficient rats (Figure 4-9A). Sprague Dawley rats were fed control or low iron diets and RNA was purified from mucosal scrapes. Equal loading of the RNA was assessed by using UN-SCAN-IT-gel-Gel Analysis Software of the image of the RNA gel (Figure 4-9A). Moreover, rats on control or iron deficient diets and IEC-6 cells were used to quantify *Atp7a* mRNA expression. The film clearly indicates induction of *Atp7a* mRNA expression in iron-deficient rat. Also, the IEC-6 cells and iron deficient lanes show different size bands (Figure 4-8B). This experiment clearly indicates the induction of the *Atp7a* gene when comparing the control and iron- deficient rats (Figure 4-8)

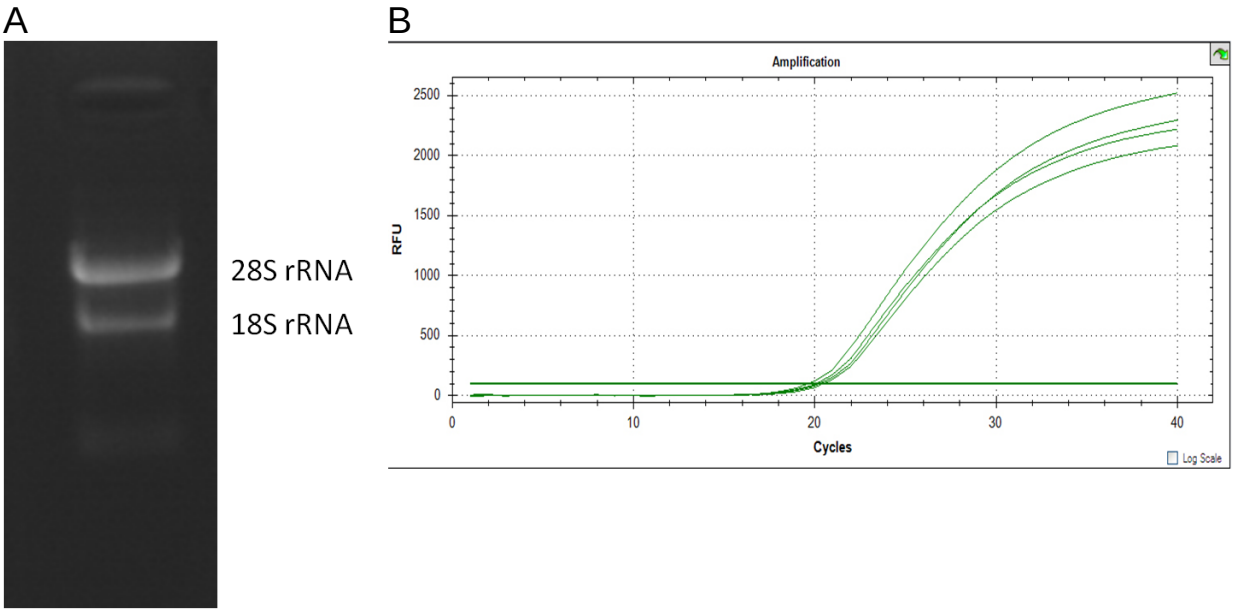

Figure 4-1. Assessment of RNA Quality. Total RNA was isolated from IEC-6 cells: Panel A, 2 µg of total RNA in agarose gel. Panel B, duplicate of 18s and exon 1 forward and 3 reverse amplication curve from qRT-PCR, showing the RNA integrity. Extensive studies in our lab had shown that intact RNA Ct value is between 18 and 20. Panel C, qRT-PCR using exon 1 forward and exon 3 reverse primer set, indication of successful cDNA synthesis as this is from the 5' end of the *Atp7a* transcript.

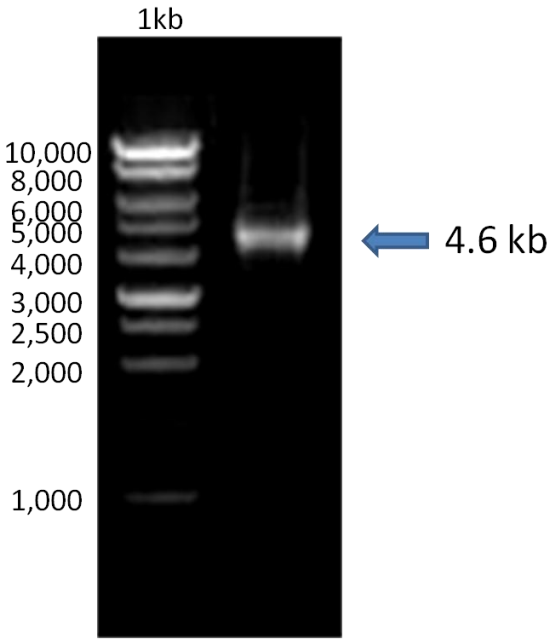

Figure 4-2. Amplification of Atp7a full-length transcript. PCR analysis of full-length Atp7a from IEC-6 cells. Primer sets were exon 1 forward and exon 23 reverse. The PCR products were loaded in 1 % agarose gel with 1 Kb ladder. The expected size of the full-length is 4,682 bp.

A

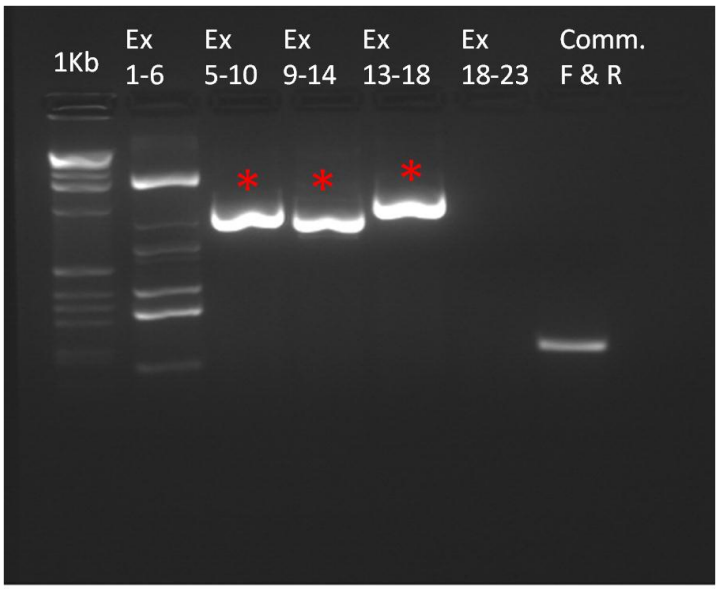

B

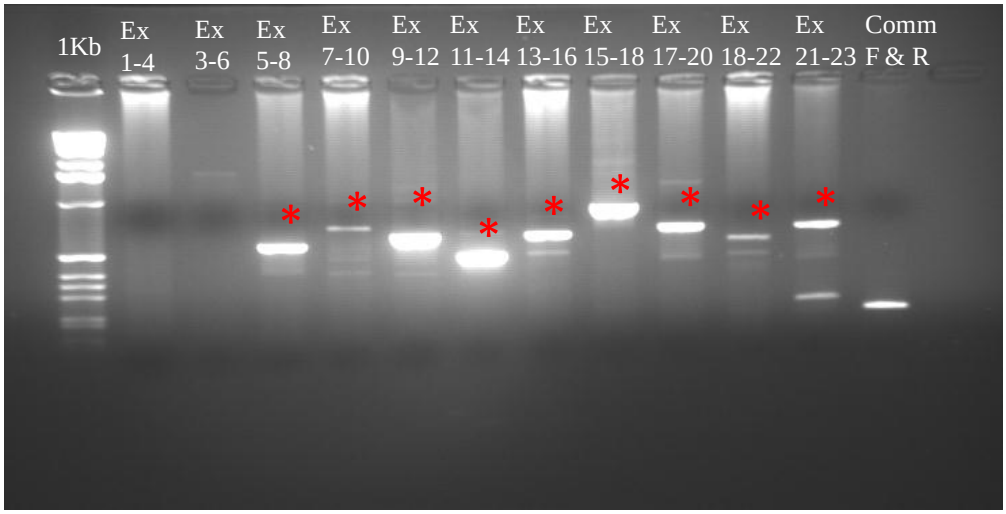

Figure 4-3. PCR analysis of different sets of exons. PCR: Panel A, the exon 1-6 lane shows multiple bands which represents splice variants. Panel B, exon 7-10, 13-16, 17-20, 18-22, and 21-23 lanes also show multiple bands which represent splice variants. Both Panel A and B are *Atp7a* from IEC-6 cells. Common F & R are loaded as the positive control. * indicates expected size bands.

A

B

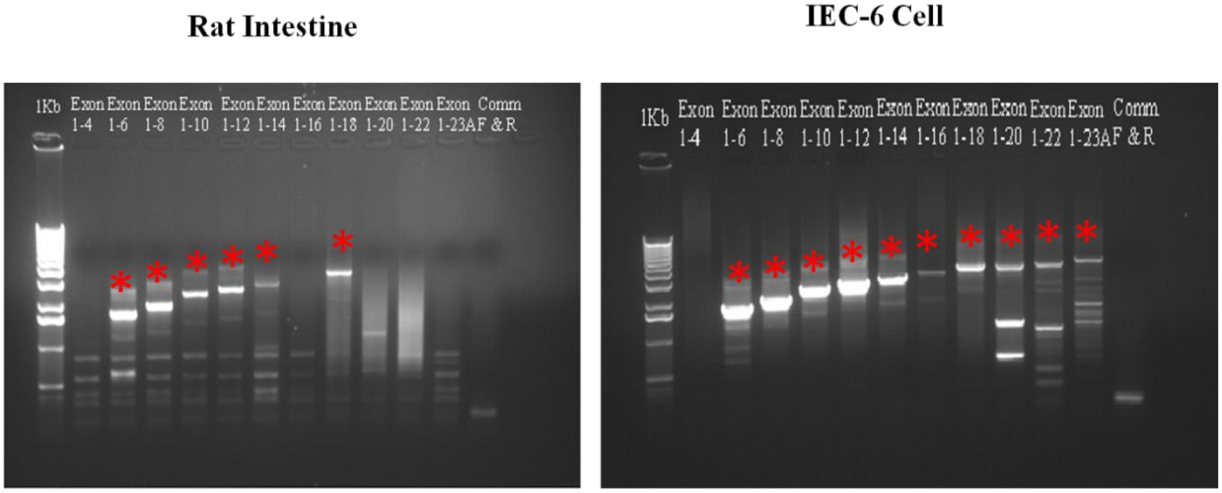

Figure 4-4. RT-PCR amplification using exon 1 forward primer in combination with various reverse primers. PCR: Panel A, total RNA isolated from rat intestine mucosal scrape. Exon 1-6, 1-8, 1-10,1-12 and 1-14 lanes show multiple bands which represent splice variants. Panel B, total RNA isolated from IEC-6 cells. Exon 1-20, 1-22, and 1-23 lanes indicate different bands. Specifically the exon 1-23 lane shows multiple transcripts. Both Panel A and B used different reverse primers and common forward and reverse primers for the positive control. * indicates expected size bands.

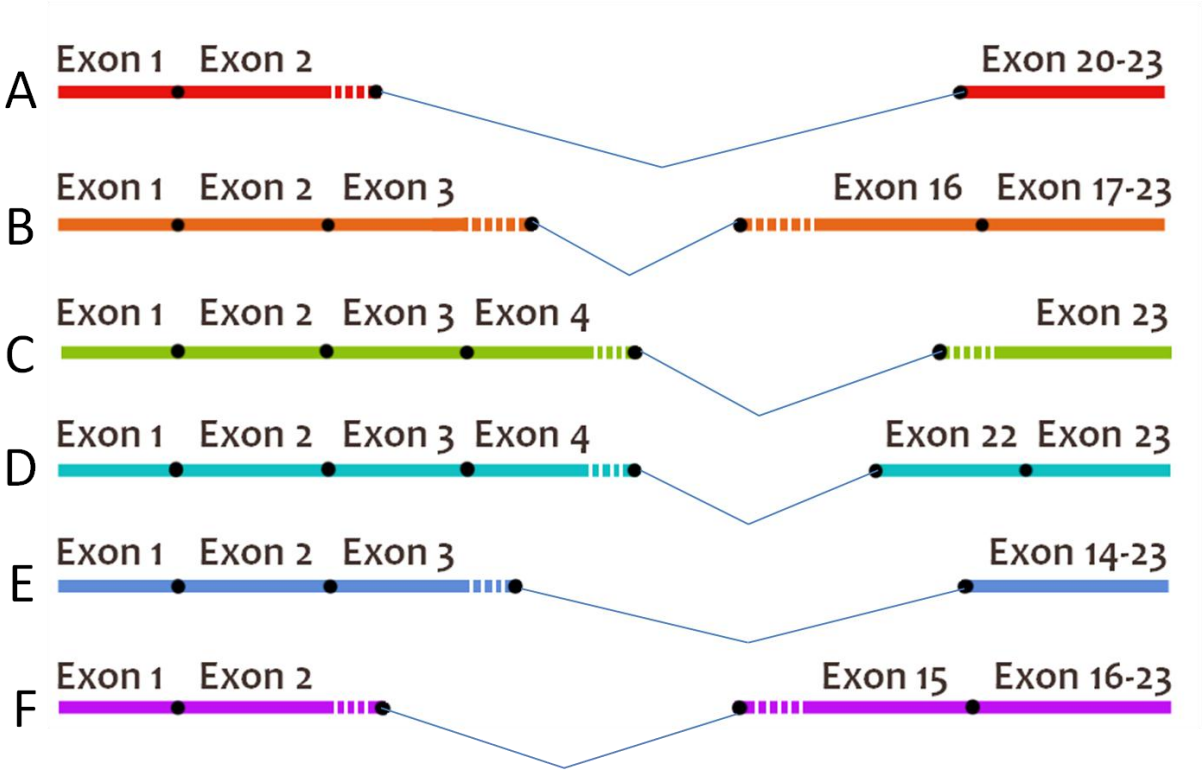

Figure 4-5. Gene structure of novel Atp7a splice variants. Indication of where splicing occurs in different exons is shown. These were amplified from IEC-6 cell RNA. Exons contained within the different transcript variants are shown. A dashed line indicates that splicing occurred within the indicated exon. The lines between the exons indicate the regions of the full-length transcript that were spliced out. Novel splice variants shown in this figure were derived from cloning of the PCR products using Ex 1-23 primers in IEC-6 cells and these bands came from series of experiments. An example of one of these experiments is shown in figure 4-4 panel B (Exon 1-23A).

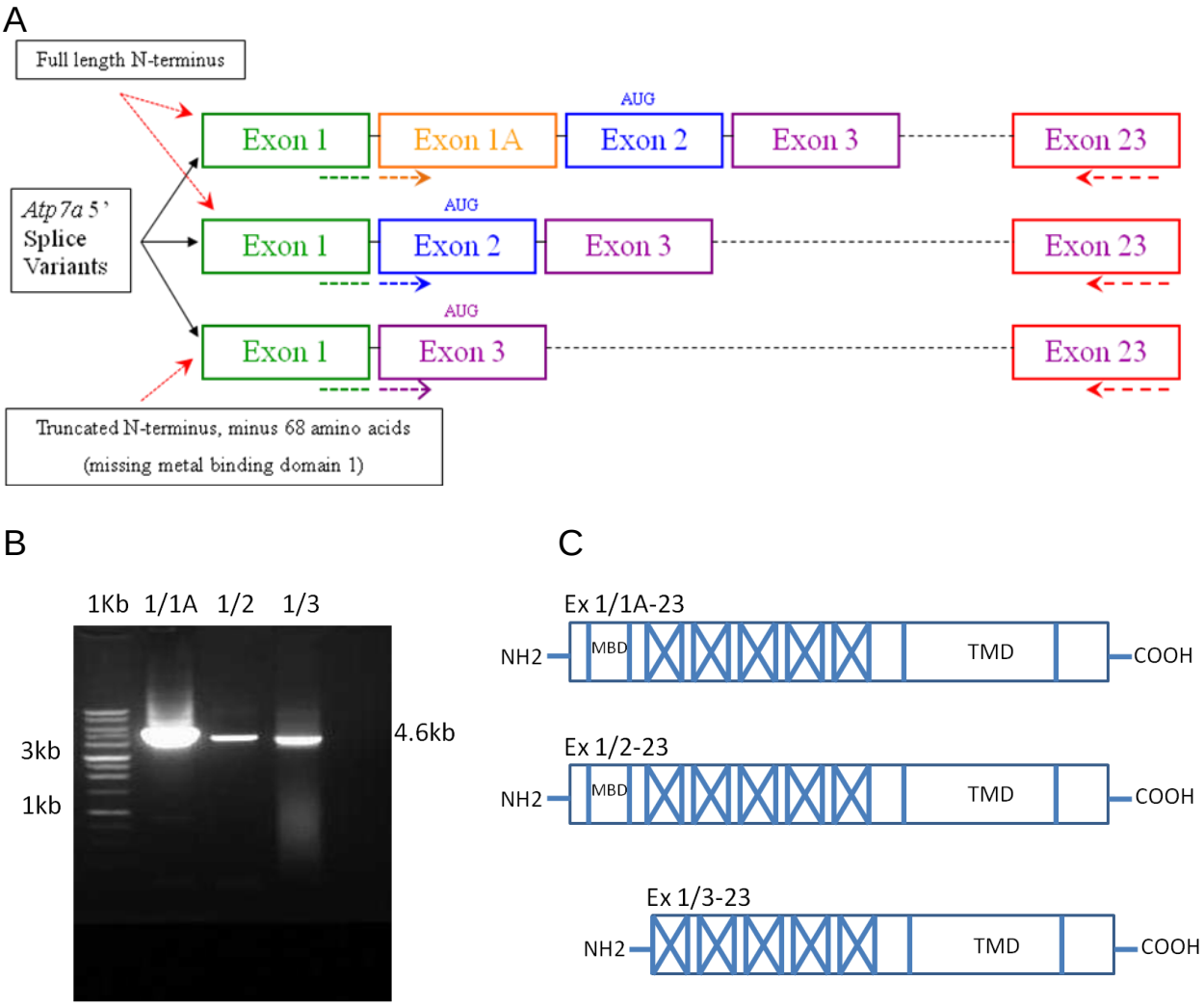

Figure 4-6. Amplification of full-length *Atp7a* cDNAs containing 5' end splice variants. Panel A, gene structure and relative location of PCR primers. Whether these three splice variants continue to exon 23 is unknown. The 5' variants are the findings from the previous study from our lab (1). Panel B, PCR analysis using IEC-6 cells. 25 µl of Exon 1/1a, 1/2, and 1/3 PCR product were loaded in lanes 1, 2, and 3, respectively. This indicates that all three 5' end splice variants exists as full-length transcript. Panel C, schematic figure of Atp7a proteins showing functional domains of Ex1/1a,1/2, and 1/3. Ex1/1a and 1/2 is full-length, and Ex 1/3 is shorter missing metal binding domain (MBD)1. TMD-transmembrane domains.

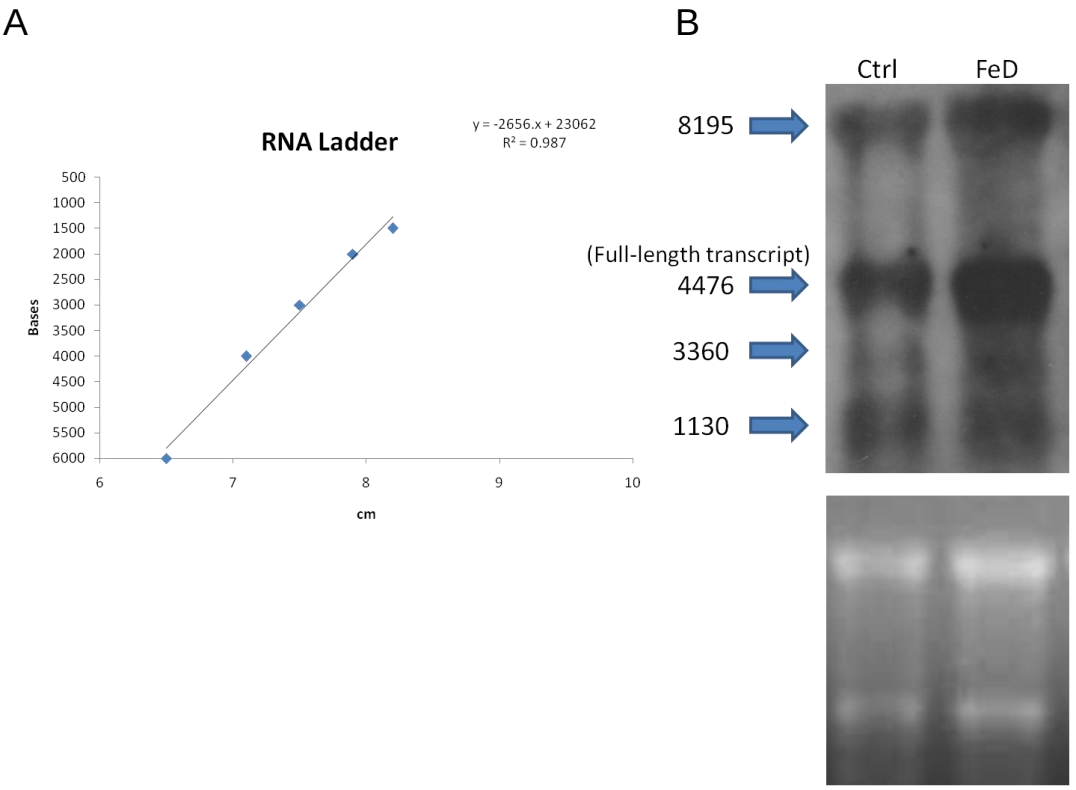

Figure 4-7. Determination of the number of different *Atp7a* transcripts. Panel A, this is regression analysis by measuring the distance of each of the bands that the ladder traveled from the top to the gel. Total RNA was isolated from SD rat mucosal scrapes. Panel B, Northern blot of control and iron deficient mucosal scrapes. 5 µg of total RNA was loaded in 1X MOPS buffer containing 2% formaldehyde agarose gel, then transferred to a nylon membrane. The blot was probed with a *Atp7a* full-length transcript. The arrows indicate the different sized transcripts that were detected under high stringency conditions. Shown below the northern blot is the stained RNA gel exemplifying equal loading.

A

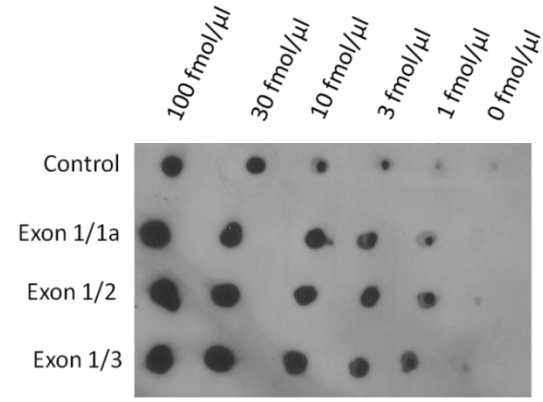

B

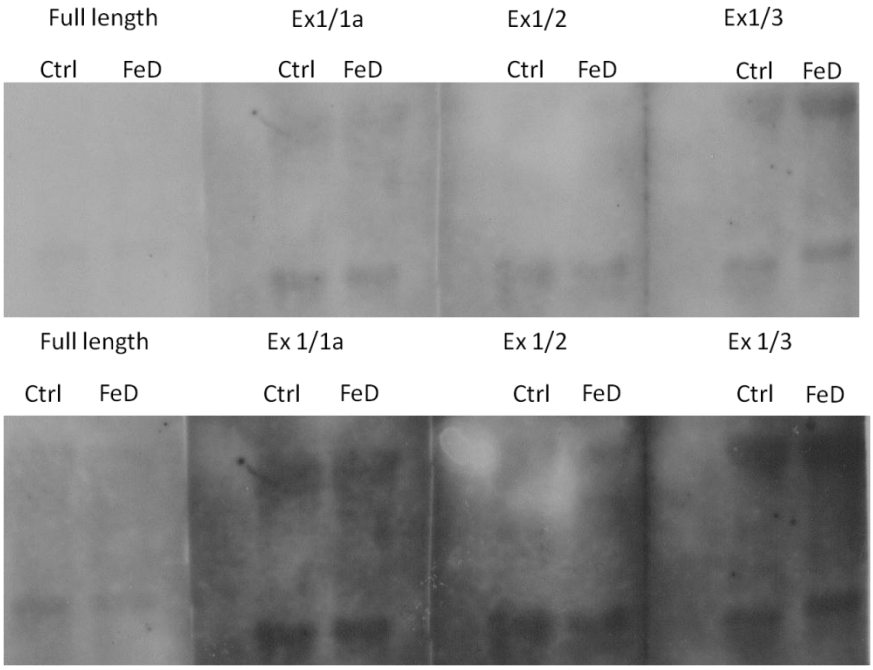

Figure 4-8. Oligonucleotide 3'end labeling of exon 1/1a, 1/2, and 1/3. Panel A, Different dilution series of the oligonucleotide was completed to see the labeling efficiency. Panel B, Total RNA was isolated from SD rat mucosal scrapes. 5 µg of total RNA were loaded in 1X MOPS buffer containing 2% formaldehyde agarose gel, then transferred to a nylon membrane. The blots were probed with either full-length or Ex1/1a, 1/2, and 1/3 that are labeled with digoxigenen-ddUTP. Short (top, panel B) and long (bottom, panel B) exposures are shown.

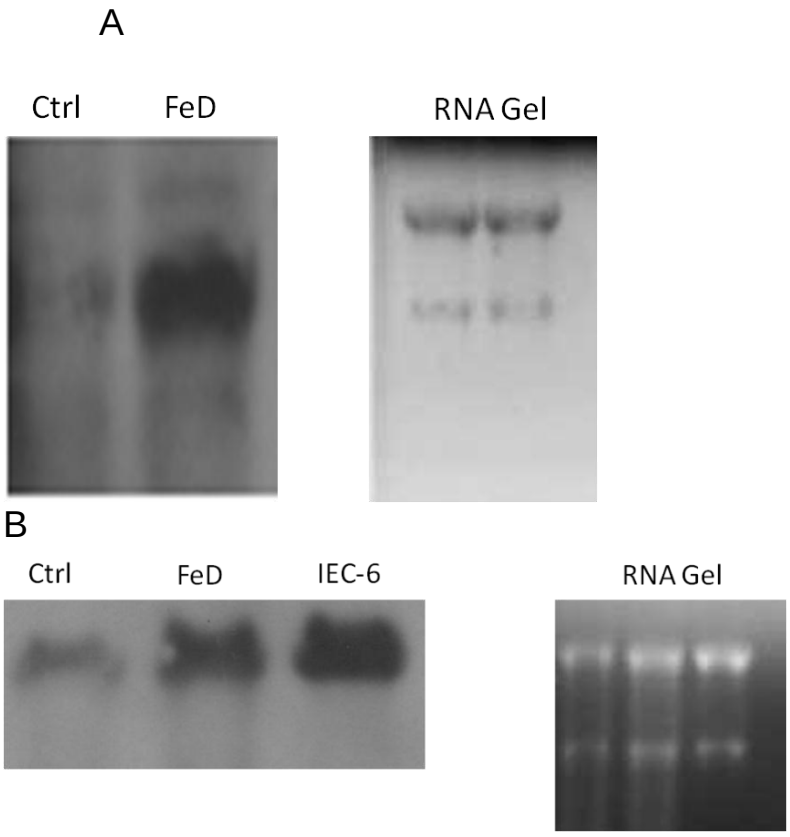

Figure 4-9. Gene expression under iron deficiency. Northern blot: Panel A, 5 µg of control and iron- deficient rat duodenum mucosal scrape RNA were loaded in 1X MOPS buffer containing 2% formaldehyde agarose gel. Panel B, the same amount of the product as panel A was loaded in addition to also loading RNA from IEC-6 cells. Both panel A and B were probed with full-length *Atp7a* PCR product. Shown next to the Northern blot is the stained RNA gel exemplifying equal loading.

CHAPTER 5
DISCUSSION

Specific Aim I

The aim of this study was to determine the composition of *Atp7a* transcript variants using a PCR based approach. The cloning and sequencing of the genes for Menkes disease has shown its importance for copper transport and homeostasis in mammalian cells (61). PCR was used to determine the structure of *Atp7a* transcript variants and to amplify full-length *Atp7a* for Northern blot experiments. In this study, intestinal epithelial cells (IEC-6) were used because we know that *Atp7a* is strongly induced by iron chelation in IEC-6 cells, which are an appropriate cell model for intestinal iron absorption.

Using RT-PCR with different primer sets, several parts of the *Atp7a* transcript were amplified to see if we detected multiple bands, indicating they are alternative splices in that region of the gene. Since *Atp7a* is such a large gene, we amplified the gene in pieces, looking for regions that contain more than one band. The exon 1-6 amplification showed multiple bands at the 5' end (Figure 4-3A). This result could indicate the presence of transcript variants. Another example of a gel showed multiple bands in exon 13-16, 18-22, and 21-23 amplifications (Figure 4-3B). These observations again suggested that there may be alternative splicing in that region. Studies done in different cell lines were thus able to show the existence of multiple forms of the ATPase. Through another recent study, the authors were able to indicate how different isoforms befit potential roles in the normal physiology of copper (61, 62). However, the physiological relevance of these variants was not clear.

In addition to these potentially novel splice variants, we were also able to identify full-length transcripts that contained the novel 5' splice variants. Through an extensive number of experiments, we eventually decided to focus on exon 1-23. We hypothesized that most transcripts would have exon 1 and exon 23 (which contained the stop codon).

PCR amplification of full-length *Atp7a* transcripts containing 5' splice variants was accomplished. Previously, 5' RACE analysis was completed to study the promoter region and to map the transcription start site, which is the 5' end of the mRNA. These PCR products were sequenced and it was determined that there were three splice variants at the 5' end of the gene (1). Using these three splice variants, forward primers were designed. The forward primers spanned different 5' exons and exon 23 reverse primers were used for this PCR amplification. The purpose of splicing is to modify the full-length Atp7a mRNA and to produce uniquely structured transcript variants that code for alternative proteins that play roles in copper transport or regulatory roles. The PCR data showed amplicons that were close to the predicted size of full-length transcript, which was ~4.6 kb (Figure 4-6B). This result indicates that all three 5' end splice variants exist as full-length transcripts.

Specific Aim II

Additionally, the Northern blot technique was use to determine the number of *Atp7a* transcripts that exist in intestinal epithelial cells and to examine *Atp7a* mRNA expression during iron deficiency. Previously, a study was done using human cell lines that expressed the Menkes Cu-transporting Atp7a. By using Northern blot analysis, they were able to find the evidence for a smaller transcript by using a probe with exon 23 sequences (60). In this study Sprague Dawley (SD) rats were used, because this rat is

an appropriate model for basic multi-purpose research, and SD rats have been used extensively by our lab in the past.

The full-length *Atp7a* was PCR was successfully amplified using exon 1 forward and exon 23 reverse primers. The size of the band showed the predicted size, which is 4.6 kb (Figure 4-2). The full- length cDNA was used as a template for generating random primed probes for Northern blot. Using the full-length probe, the Northern blot from control and iron-deficient rats showed multiple transcripts (Figure 4-7). Also, this experiment confirmed, by an independent method, that *Atp7a* mRNA is increased in the iron deficient state confirming previous results using qRT-PCR.

Next, 3'end labeled oligonucleotides were used as probes. These probes are able to detect a specific target, mainly the *Atp7a* transcript. In this experiment, a significant amount of background was observed on the images. However, an identical pattern using full-length probe vs. different oligonucleotides was noted (Figure 4-8). This finding again suggests that full-length transcripts exist containing the novel 5' splice variants.

A previous study on divalent metal transporter 1 (DMT1) splice variants was done. The experiment showed that alternative promoters and alternative RNA processing creates a combination of four DMT1 mRNA variants. One of the isoforms of DMT1 is most actively expressed in duodenal and kidney cells. Another isoform correlates with the role of DMT1 in the release of iron from endosomes, following iron uptake by the transferrin cycle (63). Having identified these different transcript and protein variants, it is now possible to address specific functions and biological roles.

In summary, by using the PCR technique and Northern blot techniques we have identified multiple *Atp7a* transcripts. Presumably, the resulting different mRNAs may be

translated into different protein isoforms. The alternative full-length transcripts shown to exist containing the novel 5’ splice variants, may also code for multiple proteins. Furthermore, by an independent method, induction of Atp7a mRNA expression in the duodenum of iron- deficient rats was confirmed.

Overall, these finding are novel and they pave the way for future studies. These PCR amplicons can be cloned into a CFP vector to produce fusion proteins that can be expressed in intestinal epithelial cells. The intracellular locations of the proteins can then be determined by confocal microscopy. It will be important to determine if these transcripts encode new protein variants and to determine the physiologic roles of these proteins.

APPENDIX
SEQUENCE DATA FOR NOVEL SPLICE VARIANTS

These are the raw sequence data for novel splice variants that are shown in Figure 4-5.

All sequences are shown 5’ to 3’. Exon 1 forward and exon 23 reverse primers are

used.

Figure 4-5. Schematic A

CTCACTATAG GGCGAATTGG GCCCTCTAGA TGCATGCTCG AGCGGCCGCC
AGTGTGATGG ATATCTGCAG AATTCGCCCT TAGGCTGCGT GCTGGTTGAT
CGCTGCCGCC CTACGGAGCT CCGAGCTCGA ACCCCAGCCC TGGAATCCTA
GGAATGTAAG GACATCAAAA TGGAACCAAA TATGGATGCA AATTCAATTA
CTATCACTGC TGAGGGAATG ACCTTCTGGA TGTTGTGGCA AGTATTGACT
TGTCAAGGAA AACAGTCAAG AGGATTCGAA TCAATTTTGT CTTTGCCCTG
ATTTATAATC TGATTGGAAT TCCCATCGCT GCTGGAGTTT TTCTGCCCAT
CGGCTTGGTT TTACAACCCT GGATGGGATC CGCAGCCGTG GCCGCTTCAT
CTGTCTCTGT GGTACTTTCT TCCCTTTTCC TCAAGCTTTA CAGGAAGCCA
ACATATGACA ATTATGAGTT GCGTCCCCGG AGCCACACAG GACAGAGGAG
TCCTTCAGAA ATCAGCGTTC ACGTTGGAAT AGATGATACC TCCAGAAATT
CTCCAAGACT GGGTTTACTG GACCGGATTG TCAATTACAG CAGAGCCTCC
ATAAATTCAC TGCTGTCTGA CAAACGCTCC CTCAACAGCG TCGTCACTAG
TGAGCCTGAT AAGCACTCAC TTCTGGTGGG AGACTTCCGG GAAGATGACG
ACACCACACT GAAGGGCGAA TTCCAGCACA CTGGCGGCCG TTACTAGTGG
ATCCGAGCTC GGTACCAAGC TTGGCGTAAT CATGGTCATA GCTGTTTCCT
GTGTGAAATT GTTATCCGCT CACAATTCCA CACAACATAC GAGCCGGAAG
CATAAAGTGT AAAGCCTGGG GTGCCTAATG AGTGAGCTAA CTCACATTAA
TTGCGTTGCG CTCACTGCCC GCTTTCCAGT CGGGAAACCT GTCGTGCCAG
CTGCATTAAT GAATCGGCCA ACGCGCGGGG AGAGGCGGTT TGCGTATTGG
GCGCTCTTCC GCTTCCTCGC

Figure 4-5. Schematic B

GACTCACTAT AGGGCGAATT GGGCCCTCTA GATGCATGCT CGAGCGGCCG
CCAGTGTGAT GGATATCTGC AGAATTCGCC CTTAGGCTGC GTGCTGGTTG
ATCGCTGCCG CCCTACGGAG CTCCGAGCTC GAACCCCAGC CCTGGATTCC
TAGGAATGTA AAGACATCAA AATGGAACCA AATATGGATG CAAATTCAAT
TACTATCACT GTTGAGGGAA TGACATGTAT TTCCTGTGTC CGGACCATTG
AGCAGCAGAT TGGGAAAGTG AATGGTGTCC ATCACATTAA AGTTTCCCTA
GAAGAAAAAA GTGAACATCC TTTAGGAGCA GCTGTAACCA AATATTCCAA
GCAGGAGCTG GACACTGAAA CCTTGGGTAC CTGCACAGAT TTCCAGGTTG
TACCCGGCTG TGGAATTAGC TGTAAAGTCA CCAATATTGA AGGTTTGCTA
CATAAGAGTA ACTTGAAGAT AGAAGAAAAT AACATTAAAA ATGCATCCCT
GGTTCAAATT GATGCAATTA ATGAACAGTC ATCACCTTCA TCGTCTATGA

TTATTGATGC TCATCTCTCG AATGCTGTTA ATACTCAGCA GTACAAAGTC
CTCATTGGTA ACCGGGAATG GATGATAAGA AATGGTCCTG TCATAAGTAA
TGATGTGGAC GAGTCTATGA TTGAACATGA AAGAAGAGGC CGGACTGCTG
TGTTGGTGAC AATCGATGGT GAACTGTGTG GCTTGATCGC TATTGCTGAT
ACTGTGAAAC CTGAGGCAGA GCTGGCTGTG CACATTCTGA AATCTAAGGG
TTTGGAAGTA GTTCTGATGA CTGGAGACAA CAGTAAAACA GCTCGGTCTA
TTGCTTCTCA GGTTGGCATT ACTAAGGTGT TTGCCGAAGT TCTGCCTTCC
ACAAAGTTGC TAAGGTGAAG CAGCTTCAGG AGGAGGGAAA GCGCGCAGCC
ATGGTAGGAG ATGGAATCAA TGACTCTCCA GCTCTGGCAA TGGCAAGCGT
CGGAATTGCC ATCGG

Figure 4-5. Schematic C

GACTCACTAT AGGGCGAATT GGGCCCTCTA GATGCATGCT CGAGCGGCCG
CCAGTGTGAT GGATATCTGC AGAATTCGCC CTTAGGCTGC GTGCTGGTTG
ATCGCTGCCG CCCTACGGAG CTCCGAGCTC GAACCCCAGC CCTGGAATCC
TAGGAATGTA AAGACATCAA AATGGAACCA AATATGGATG CAAATTCAAT
TACTATCACT GTTGAGGGAA TGACATGTAT TTCCTGTGTC CGGACCATTG
AGCAGCAGAT TGGGAAAGTG AATGGTGTCC ATCACATTAA AGTTTCCCTA
GAAGAAAAAA GTGCAACTGT TATTTATAAC CCTAAACTTC AGACTCCAAA
GACCCTCCAA GAAGCTATCG ATGACATGGG CTTTGATGCT CTTCTTCACA
ATGCTAACCC TCTTCCTGTC TTAACCAATA CTGTGTTTCT GACTGTTACT
GCTCCACTGG CTCTGCCATG GGACCATATC CAAAGTACAT TGCTCAAGAC
CAAGGGTGTG ACTGGGGTTA AGATTTCCCC TCAGCAAAGA AGTGCAGTGG
TTACCATAAT CCCATCTGTG GTGAGTGCTA ATCAGATCGT GGAGCTGGTC
CCAGACCTCA GTTTAGACAT GGGAACTCAG GAGAAAAAGT CAGGAACTTC
TGAGGAGCAT AGCACACCTC AGGCAGGGGA AGTCCCGCTG AAGATGAGAG
TGGAAGGGAT GACCTGCCTT TCATGCACTA GCACCATTGA AGGAAAAGTT
GGAAAGCTGC AAGGTGTACA ACGCATTAAA GTGTCCCTAG ACAACCAAGA
AGCTACTATT GTGTATCAAC TTCATCTGTC TCTGTGGTAC TTTCTTCCCT
TTTCCTCAAG CTTTACAGGA AGCCAACATA TGACAATTAT GAGTTGCGTC
CCCGGAGCCA CACAGGACAG AGGAGTCCTT CAGAAATCAG CGTTCACGTT
GGAATAGATG ATACCTCCAG AAATTCTCCA TGACTGGGTT TACTGGACCG
GATTGTCAAT TACAGCAGAG CCTCCA

Figure 4-5. Schematic D

GACTCACTAT AGGGCGAATT GGGCCCTCTA GATGCATGCT CGAGCGGCCG
CCAGTGTGAT GGATATCTGC AGAATTCGCC CTTAGGCTGC GTGCTGGTTG
ATCGCCGCCG CCCTACGGAG CTCCGAGCTC GAACCCCAGC CCTGGAATCC
TAGGAATGTA AAGACATCAA AATGGAACCA AATATGGATG CAAATTCAAT
TACTATCACT GTTGAGGGAA TGACATGTAT TTCCTGTGTC CGGACCATTG
AGCAGCAGAT TGGGAAAGTG AATGGTGTCC ATCACATTAA AGTTTCCCTA
GAAGAAAAAA GTGCAACTGT TATTTATAAC CCTAAACTTC AGACTCCAAA

GACCCTCCAA GAAGCTATCG ATGACATGGG CTTTGATGCT CTTCTTCACA
ATGCTAACCC TCTTCCTGTC TTAACCAGTA CTGTGTTTCT GACTGTTACT
GCTCCACTGG CTCTGCCATG GGACCATATC CAAAGTACAT TGCTCAAGAC
CAAGGGTGTG ACTGGGGTTA AGATTTCCCC TCAGCAAAGA AGTGCAGTGG
TTACCATAAT CCCATCTGTG GTGAGTGCTA ATCAGATCGT GGAGCTGGTC
CCAGACCTCA GTTTAGACAT GGGAACTCAG GAGAAAAAGT CAGGAACTTC
TGAAGAGCAT AGCACACCTC AGGCAGGGGA AGTCCTGCTG AAGATGAGAG
TGGAAGGGAT GACCTGCCAT TCATGCACTA GCACCATTGA AGGAAAAGTT
GGAAAGCTGC AAGGTGTACA ACGCATTAAA GTGTCCCTAG ACAACCAAGA
AGCTACTATT GTGTATCAAC CTCATCTGAT CACAGCAGAG GAAATAAAGA
AGCAGATTGA AGCTGTGGGT TTTCCAGCCT TCATAAAAAA ACAGCCAAAG
TACCTCAAAT TGGGAGCCAT TGACGTTGAG CGCCTGAAGA GTACACCAGT
CAAATCTTCA GAAGGATCTC AGCAAAAGAG CCCAGCGTAT CCCAGTGACT
CAGCAATCAC ATTTACCATA GACGGCATGC ATT

Figure 4-5. Schematic E

GACTCACTAT AGGGCGAATT GGGCCCTCTA GATGCATGCT CGAGCGGCCG
CCAGTGTGAT GGATATCTGC AGAATTCGCC CTTAGGCTGC GTGCTGGTTG
ATCGCTGCCG CCCTACGGAG CTCCGAGCTC GAACCCCAGC CCTGGAATCC
TAGGAATGTA AAGACATCAA AATGGAACCA AATATGGATG CAAATTCAAT
TACTATCACT GTTGAGGGAA TGACATGTAT TTCCTGTGTC CGGACCATTG
AGCAGCAGAT TGGGAAAGTG AATGGTGTCC ATCACATTAA AGTTTCCCTA
GAAGAAAAAA GTGCAACTGT TATTTATAAC CCTAAACTTC AGACTCCAAA
GGCTCCTATC CAGCAGTTTG CAGACAAACT CAGTGGCTAC TTTGTTCCTT
TTATCGTCTT GGTTTCCATT GTTACCCTCT TGGTGTGGAT TATAATTGGA
TTTCAAAATT TTGGAATTGT GGAAGCCTAC TTTCCCGGCT ACAACAGAAG
CATCTCCCGA ACAGAAACCA TAATCCGCTT TGCTTTCCAA GTGTCTATCA
CAGTTCTGTG TATCGCATGT CCCTGTTCAC TGGGGCTAGC CACCCCAACT
GCTGTGATGG TGGGCACAGG AGTAGGTGCT CAGAATGGCA TACTTATCAA
AGGTGGGGAG CCACTGGAGA TGGCTCATAA GGTAAAGGTA GTGGTGGTTG
ACAAGACTGG AACCATTACC CATGGAACCC CAGTAGTGAA CCAAGTAAAG
GTTCAGGTGG AAAGTAACAA GATATCACGC AATAAGATCC TGGCCATTGT
GGGAACTGCA GAAAGTAACA GTGAACATCC TTTAGGAGCA GCTGTAACCA
AATATTGCAA GCAGGAGCTG GACACTGAAA CCTTGGGTAC CTGCACAGAT
TTCCAGGTTG TACCCGGCTG TGGAATTAGC TGTAAAGTCA CCAATATTGA
AGGTTTGCTA CATAAGAGTA ACTTGAAGAT AGAAGAAAAT AACATTAAAA
ATGCATCCCT GGTTCAAA

Figure 4-5. Schematic F

GACTCACTAT AGGGCGAATT GGGCCCTCTA GATGCATGCT CGAGCGGCCG
CCAGTGTGAT GGATATCTGC AGAATTCGCC CTTAGGCTGC GTGCTGGTTG
ATCGCTGCCG CCCTACGGAG CTCCGAGCTC GAACCCCAGC CCTGGAATCC

TAGGAATGTA AAGACATCAA AATGGAACCA AATATGGATG CAAATTCAAT
TACTATCACT GTTGAGGGAA TGACATGTAT TTCCTGTGTC CGGACCATTG
AGCAGCAGAT TGGGAAAGTA ACAAGATATC ACGCAATAAG ATCCTGGCCA
TTGTGGGAAC TGCAGAAAGT AACAGTGAAC ATCCTTTAGG AGCAGCTGTA
ACCAAATATT GCAAGCAGGA GCTGGACACT GAAACCTTGG GTACCTGCAC
AGATTTCCAG GTTGTACCCG GCTGAGGAAT TAGCTGTAAA GTCAGCAATA
TTGAAGGTTT GCTACATAAG AGTAACTTGA AGATAGAAGA AAATAACATT
AAAAATGCAT CCCTGGTTCA AATTGATGCA ATTAATGAAC AGTCATCACC
TTCATCGTCT ATGATTATTG ATGCTCATCT CTCAAATGCT GTTAATACTC
AGCAGTACAA AGTCCTCATT GGTAACCGGG AATGGATGAT TAGAAATGGT
CTTGTCATAA GTAATGATGT GGACGAGTCT ATGATTGAAC ATGAAAGAAG
AGGCCGGACT GCTGTGTTGG TGACAATCGA TGATGAACTG TGTGGCTTGA
TCGCTATCGC TGATACTGTG AAACCTGAGG CAGAGCTGGC TGTGCACATT
CTGAAATCTA TGGGTTTGGA AGTAGTTCTG ATGACTGGAG ACAACAGTAA
AACAGCTCGG TCTATTGCTT CTCAGGTTGG CATTACTAAG GTGTTTGCCC
GAAGTTCTGC CTTCCCACAA GTTGCTAAGG TGAAGCAGCT TCAGGAGGAG
GGAAAGCGCG TAGCCATGGT AGGAGATGGA ATCAATGACT CTCCAGCTCT
GGCAATGG

REFERENCES

1. Collins JF, Hua P, Lu Y, Ranganathan PN. Alternative splicing of the Menkes copper Atpase (Atp7a) transcript in the rat intestinal epithelium. Am J Physiol-Gastr L 2009;297(4):G695-G707.

2. Fox PL. The copper-iron chronicles: The story of an intimate relationship. Biometals 2003;16(1):9-40.

3. Hart EB SH, Elvehjem CA. Iron in nutrition. I. Nutritional anemia on whole milk diets and the utilization of inorganic iron in hemoglobin building. J Biol Chem 1925;65:67-80.

4. Sherman AR, Moran PE. Copper-Metabolism in Iron-Deficient Maternal and Neonatal Rats. J Nutr 1984;114(2):298-306.

5. Gambling L, Dunford S, McArdle HJ. Iron deficiency in the pregnant rat has differential effects on maternal and fetal copper levels. J Nutr Biochem 2004;15(6):366-72.

6. Collins JF, Franck CA, Kowdley KV, Ghishan FK. Identification of differentially expressed genes in response to dietary iron deprivation in rat duodenum. Am J Physiol-Gastr L 2005;288(5):G964-G71.

7. Sheth S, Brittenham GM. Genetic disorders affecting proteins of iron metabolism: Clinical implications. Annu Rev Med 2000;51:443-64.

8. Testa U, ed. Proteins of Iron Metabolism Boca Raton, Fl: CRC Press, 2002.

9. Werman MJ, Barat E, Bhathena SJ. Gender, Dietary Copper and Carbohydrate Source Influence Cardiac Collagen and Lysyl Oxidase in Weanling Rats. J Nutr 1995;125(4):857-63.

10. Prohaska JR. Biochemical-Changes in Copper Deficiency. J Nutr Biochem 1990;1(9):452-61.

11. Milne DB. Assessment of Copper Nutritional-Status. Clin Chem 1994;40(8):1479-84.

12. Bonham M, O'Connor JM, Hannigan BM, Strain JJ. The immune system as a physiological indicator ofmarginal copper status? Brit J Nutr 2002;87(5):393-403.

13. Xie L, Collins JF. Transcriptional regulation of the Menkes copper ATPase (Atp7a) gene by hypoxia-inducible factor (HIF2{alpha}) in intestinal epithelial cells. Am J Physiol Cell Physiol 2011;300(6):C1298-305.

14. van den Berghe PVE, Klomp LWJ. New developments in the regulation of intestinal copper absorption. Nutr Rev 2009;67(11):658-72.

15. Menkes JH, Weakley DR, Alter M, Steigleder GK, Sung JH. Sex-Linked Recessive Disorder with Retardation of Growth, Peculiar Hair, and Focal Cerebral and Cerebellar Degeneration. Pediatrics 1962;29(5):764-&.

16. Lutsenko S, Petris NJ. Function and regulation of the mammalian copper-transporting ATPases: Insights from biochemical and cell biological approaches. J Membrane Biol 2003;191(1):1-12.

17. Recommended dietary allowances--1980. Nutr Rev 1980;38(8):290-4.

18. Gaetke LM, Chow CK. Copper toxicity, oxidative stress, and antioxidant nutrients. Toxicology 2003;189(1-2):147-63.

19. Lurie DG HJ, Schubert A. . Journal of Food Composition and Analysis 1989;2:298-316.

20. Institute of Medicine. Copper. In: Food and Nutrition Board e. Dietary Reference Intakes: Vitamin A, Vitamin K, Arsenic, Boron, Chromium, Copper, Iodine, Iron, Manganese, Molybdenum, Nickel, Silicon, Vanadium, and Zinc. . Washington, DC: National Academy Press, 2002:224-57.

21. Trumbo P, Yates AA, Schlicker S, Poos M. Dietary reference intakes: Vitamin A, vitamin K, arsenic, boron, chromium, copper, iodine, iron, manganese, molybdenum, nickel, silicon, vanadium, and zinc. J Am Diet Assoc 2001;101(3):294-301.

22. Haschke F, Ziegler EE, Edwards BB, Fomon SJ. Effect of Iron Fortification of Infant Formula on Trace Mineral Absorption. J Pediatr Gastr Nutr 1986;5(5):768-73.

23. Linder MC, Zerounian NR, Moriya M, Malpe R. Iron and copper homeostasis and intestinal absorption using the Caco2 cell model. Biometals 2003;16(1):145-60.

24. Dancis A, Yuan DS, Haile D, et al. Molecular Characterization of a Copper Transport Protein in Saccharomyces-Cerevisiae - an Unexpected Role for Copper in Iron Transport. Cell 1994;76(2):393-402.

25. Zhou B, Gitschier J. hCTR1: A human gene for copper uptake identified by complementation in yeast. P Natl Acad Sci USA 1997;94(14):7481-6.

26. Nose Y, Kim BE, Thiele DJ. Ctr1 drives intestinal copper absorption and is essential for growth, iron metabolism, and neonatal cardiac function. Cell Metab 2006;4(3):235-44.

27. Gunshin H, Fujiwara Y, Custodio AO, DiRenzo C, Robine S, Andrews NC. Slc11a2 is required for intestinal iron absorption and erythropoiesis but dispensable in placenta and liver. J Clin Invest 2005;115(5):1258-66.

28. Gunshin H, Mackenzie B, Berger UV, et al. Cloning and characterization of a mammalian proton-coupled metal-ion transporter. Nature 1997;388(6641):482-8.

29. Arredondo M, Munoz P, Mura CV, Nunez MT. DMT1, a physiologically relevant apical Cu1+ transporter of intestinal cells. Am J Physiol-Cell Ph 2003;284(6):C1525-C30.

30. Ravia JJ, Stephen RM, Ghishan FK, Collins JF. Menkes copper ATPase (Atp7a) is a novel metal-responsive gene in rat duodenum, and immunoreactive protein is present on brush-border and basolateral membrane domains. J Biol Chem 2005;280(43):36221-7.

31. Knopfel M, Smith C, Solioz M. ATP-driven copper transport across the intestinal brush border membrane. Biochem Bioph Res Co 2005;330(3):645-52.

32. Bremner I. Involvement of Metallothionein in the Hepatic-Metabolism of Copper. J Nutr 1987;117(1):19-29.

33. Percival SS, Harris ED. Copper Transport from Ceruloplasmin - Characterization of the Cellular Uptake Mechanism. Am J Physiol 1990;258(1):C140-C6.

34. Linder MC, HazeghAzam M. Copper biochemistry and molecular biology. Am J Clin Nutr 1996;63(5):S797-S811.

35. Danks DM. Copper Deficiency in Humans. Annual Review of Nutrition 1988;8:235-57.

36. Puig S, Thiele DJ. Molecular mechanisms of copper uptake and distribution. Curr Opin Chem Biol 2002;6(2):171-80.

37. Andrews NC, Schmidt PJ. Iron homeostasis. Annu Rev Physiol 2007;69:69-85.

38. Fleming MD, Trenor CC, Su MA, et al. Microcytic anaemia mice have a mutation in Nramp2, a candidate iron transporter gene. Nat Genet 1997;16(4):383-6.

39. McKie AT, Barrow D, Latunde-Dada GO, et al. An iron-regulated ferric reductase associated with the absorption of dietary iron. Science 2001;291(5509):1755-9.

40. Latunde-Dada GO, Van der Westhuizen J, Vulpe CD, Anderson GJ, Simpson RJ, McKie AT. Molecular and functional roles of duodenal cytochrome B (Dcytb) in iron metabolism. Blood Cells Mol Dis 2002;29(3):356-60.

41. Gunshin H, Starr CN, DiRenzo C, et al. Cybrd1 (duodenal cytochrome b) is not necessary for dietary iron absorption in mice. Blood 2005;106(8):2879-83.

42. Collins JF, Prohaska JR, Knutson MD. Metabolic crossroads of iron and copper. Nutr Rev 2010;68(3):133-47.

43. Donovan A, Brownlie A, Zhou Y, et al. Positional cloning of zebrafish ferroportin1 identifies a conserved vertebrate iron exporter. Nature 2000;403(6771):776-81.

44. Pietrangelo A. Non-HFE hemochromatosis. Hepatology 2004;39(1):21-9.

45. Donovan A, Lima CA, Pinkus JL, et al. The iron exporter ferroportin/Slc40a1 is essential for iron homeostasis. Cell Metab 2005;1(3):191-200.

46. Vulpe CD, Kuo YM, Murphy TL, et al. Hephaestin, a ceruloplasmin homologue implicated in intestinal iron transport, is defective in the sla mouse. Nat Genet 1999;21(2):195-9.

47. Knutson MD, Oukka M, Koss LM, Aydemir F, Wessling-Resnick M. Iron release from macrophages after erythrophagocytosis is up-regulated by ferroportin 1 overexpression and down-regulated by hepcidin. P Natl Acad Sci USA 2005;102(5):1324-8.

48. Nicolas G, Bennoun M, Devaux I, et al. Lack of hepcidin gene expression and severe tissue iron overload in upstream stimulatory factor 2 (USF2) knockout mice. P Natl Acad Sci USA 2001;98(15):8780-5.

49. Nicolas G, Bennoun M, Porteu A, et al. Severe iron deficiency anemia in transgenic mice expressing liver hepcidin. P Natl Acad Sci USA 2002;99(7):4596-601.

50. Harris ZL, Durley AP, Man TK, Gitlin JD. Targeted gene disruption reveals an essential role for ceruloplasmin in cellular iron efflux. P Natl Acad Sci USA 1999;96(19):10812-7.

51. Prohaska JR, Gybina AA. Rat brain iron concentration is lower following perinatal copper deficiency. J Neurochem 2005;93(3):698-705.

52. Josephs HW. Studies on iron metabolism and the influence of copper. J Biol Chem 1932;96(2):559-71.

53. Marston HR, Allen SH. Function of Copper in Metabolism of Iron. Nature 1967;215(5101):645-&.

54. Collins JF. Gene chip analyses reveal differential genetic responses to iron deficiency in rat duodenum and jejunum. Biol Res 2006;39(1):25-37.

55. Dierick HA, Ambrosini L, Spencer J, Glover TW, Mercer JFB. Molecular-Structure of the Menkes Disease Gene (Atp7a). Genomics 1995;28(3):462-9.

56. Dierick HA, Adam AN, EscaraWilke JF, Glover TW. Immunocytochemical localization of the Menkes copper transport protein (ATP7A) to the trans-Golgi network. Hum Mol Genet 1997;6(3):409-16.

57. Lareau LF, Green RE, Bhatnagar RS, Brenner SE. The evolving roles of alternative splicing. Curr Opin Struc Biol 2004;14(3):273-82.

58. Bingham PM, Chou TB, Mims I, Zachar Z. On Off Regulation of Gene-Expression at the Level of Splicing. Trends Genet 1988;4(5):134-8.

59. Das S, Levinson B, Vulpe C, Whitney S, Gitschier J, Packman S. Similar Splicing Mutations of the Menkes Mottled Copper-Transporting Atpase Gene in Occipital Horn Syndrome and the Blotchy Mouse. Am J Hum Genet 1995;56(3):570-6.

60. Reddy MCM, Harris ED. Multiple transcripts coding for the Menkes gene: Evidence for alternative splicing of Menkes mRNA. Biochem J 1998;334:71-7.

61. Harris ED, Qian YC, Reddy MCM. Genes regulating copper metabolism. Mol Cell Biochem 1998;188(1-2):57-62.

62. Harris ED, Reddy MCM, Majumdar S, Cantera M. Pretranslational control of Menkes disease gene expression. Biometals 2003;16(1):55-61.

63. Hentze MW, Hubert N. Previously uncharacterized isoforms of divalent metal transporter (DMT)-1: Implications for regulation and cellular function. P Natl Acad Sci USA 2002;99(19):12345-50.

BIOGRAPHICAL SKETCH

Changae Kim was born in Anyang, South Korea and moved to the United States when she was 9 years old. Changae completed her B.S. in biology at the Northeastern Illinois University in 2007. She was married in the year of 2008 and she moved to Florida. Changae has always had a profound interest in nutrition education and research. In 2009, Changae was accepted into the M.S. program in food science and human nutrition with a concentration in nutritional sciences at the University of Florida. Currently, Changae is working under the guidance of Dr. James F. Collins. After graduation Changae intends on pursuing a doctor of philosophy in nutritional science.